NOTICE

The quality of this microfiche is heavily dependent upon the quality of the original thesis submitted for microfilming. Every effort has been made to ensure the highest quality of reproduction possible.

If pages are missing, contact the university which granted the degree.

Some pages may have indistinct print especially if the original pages were typed with a poor typewriter ribbon or if the university sent us a poor photocopy.

Previously copyrighted materials (journal articles, published tests, etc.) are not filmed.

Reproduction in full or in part of this film is governed by the Canadian Copyright Act, R.S.C., 1970, c. C-30. Please read the authorization forms which accompany this thesis.

THIS DISSERTATION
HAS BEEN MICROFILMED
EXACTLY AS RECEIVED

AVIS

La qualité de cette microfiche dépend grandement de la qualité de la thèse soumise au microfilmage. Nous avons tout fait pour assurer une qualité supérieure de reproduction.

S'il manque des pages, veuillez communiquer avec l'université qui a conféré le grade.

La qualité d'impression de certaines pages peut laisser à désirer, surtout si les pages originales ont été dactylographiées à l'aide d'un ruban usé ou si l'université nous a fait parvenir une photocopie de mauvaise qualité.

Les documents qui font déjà l'objet d'un droit d'auteur (articles de revue, examens publiés, etc.) ne sont pas microfilmés.

La reproduction, même partielle, de ce microfilm est soumise à la Loi canadienne sur le droit d'auteur, SRC 1970, c. C-30. Veuillez prendre connaissance des formules d'autorisation qui accompagnent cette thèse.

LA THÈSE A ÉTÉ
MICROFILMÉE TELLE QUE
NOUS L'AVONS REÇUE

A STUDY OF COUPLED TORSIONAL-TRANSLATIONAL RESPONSE OF BUILDINGS TO EARTHQUAKE LOADINGS

HENRY ALEXANDER GORDON

A DISSERTATION

in

The Faculty

of

Engineering

Presented in Partial Fulfillment of the Requirements
for the degree of Master of Engineering at
Concordia University
Montréal, Québec, Canada

May, 1978

ABSTRACT

ABSTRACT

A STUDY OF COUPLED TORSIONAL-TRANSLATIONAL RESPONSE OF BUILDINGS TO EARTHQUAKE LOADINGS

Henry Alexander Gordon

Torsional coupling in three-dimensional systems may be caused by the non-coincidence of the centers of mass and rigidity. This coupling is also amplified where the ratio of the fundamental frequencies in torsion and translation approach one.

A study, based on ideally elastic behavior, shows that geometric and stiffness layouts affect the sensitivity of structures with respect to coupled response.

The National Building Code requirements to account for the effects of torsion, in both the psuedo-static and dynamic analysis procedures are demonstrated.

The validity of modal spectrum analysis techniques for three-dimensional coupled analysis, is shown to be questionable in the vicinity of period coincidence. The effects of both eccentricity and period coincidence are shown to be significantly different from normal expectations and a time history analysis is recommended for coupled analysis in the vicinity of period coincidence.

ACKNOWLEDGEMENTS

ACKNOWLEDGEMENTS

I wish to thank my supervisor, Dr. O.A. Pekau for his guidance and encouragement in the preparation of this work.

I would also like to thank Concordia University and the Aluminum Company of Canada for their financial assistance during the course of my studies.

Thanks also, to my friends and family for their help and patience.

TABLE OF CONTENTS

TABLE OF CONTENTS

LIST OF TABLES

LIST OF TABLES

LIST OF FIGURES

LIST OF FIGURES

NOMENCLATURE

NOMENCLATURE

a,b	dimensions in the x and y-direction respectively
A	horizontal design ground acceleration
c	seismic wave speed
C_{ij}	damping coefficient between i and j floors
D_N	plan dimension in the direction under consideration
e_D	design eccentricity
e_x, e_y	eccentricity in the x and y-direction respectively
F	foundation factor
G	acceleration due to gravity
I	importance factor
i,j	subscript representing $i^{\underline{th}}$ and $j^{\underline{th}}$ floors
J	polar moment of inertia
K	stiffness factor
k_x, k_y	unit stiffness in x and y-direction respectively
K_x, K_y, K_θ	total stiffness in x,y and θ-directions respectively
M	mass
m	unit mass
M_{ti}	torsional moment at level i
N	number of stories
P_{ij}	lateral storey forces for level i in $j^{\underline{th}}$ mode
q	generalized coordinates

r	radius of gyration
S	seismic coefficient
V	total lateral seismic force
V_t	torsional frame shear
W	weight of structure
x,y	coordinates
$\ddot{x},\ddot{y}$	accelerations in x and y-directions respectively
$\ddot{u}_x,\ddot{u}_y$	ground acceleration in x and y-directions
α	incident angle
γ_j	modal participation factor $j^{\underline{th}}$ mode
δ	ratio of eccentricity to radius of gyration
θ	rotational angle
$\ddot{\theta}$	rotational acceleration
ψ	degree of coupling
ϕ_n	$n^{\underline{th}}$ mode shape
ϕ	mode shape
λ	natural frequency squared
ρ	mass density
ω	natural circular frequency
ω'_θ,ω'_y	associated natural symmetric frequencies

CHAPTER I

INTRODUCTION

CHAPTER I

INTRODUCTION

Observations, after recent earthquakes, have uncovered structural member failures due to the torsional motions of buildings [6]. In less severe circumstances, wind induced torsional-translational oscillations have caused considerable damage to the Hancock Tower in Boston [4]. In order to more fully understand these situations, this study investigates, in part, the causes and effects of coupled torsional-translational motions of dynamic systems.

The general approach to dynamic analysis of structural response is to consider independently the two orthogonal directions of a structure and analyze each separately. Such an analysis is valid for systems with coincident centers of mass and resistance. When the centers of mass and resistance are not coincident, coupling between torsional and translational motions exists.

Ayre [1] was one of the first to examine this concept and was followed by others [7, 8, 12, 15, 19, 23]. However, other researchers have reported different situations, which could cause coupling and torsional motions. Newmark [17] as well as others [7,14] reported on the spatial concept of seismic waves. Newmark reasoned, that since velocity of seismic wave propagation, is a finite quantity, non-synchro-

nous motion of different contact points on a structure could induce torsional motions. Hart and Dijulio [7] arrived at the following equation, using a similar approach.

$$\ddot{\theta}(t) = \frac{1}{2C} [\ddot{u}_x(t)\sin\alpha - \ddot{u}_y(t)\cos\alpha] \qquad (1.1)$$

where $\ddot{u}_x$ and $\ddot{u}_y$ represent ground accelerations in the x and y directions respectively, C the seismic wave velocity and α the incident angle. Thus, translational accelerations, alone, distinct from dynamic assymmetry, may excite torsional response.

Tso [24,25] proposed that torsional response arise as a result of non-linear coupling between translational and torsional motions, the coupling being caused by the non-linear force-displacement characteristics of the restoring forces of the structure. Tso and Asmis [25] considered the response of a single mass system, based on numerical analysis. Tso [24] later presented an analytical study of the problem, after simplifying certain parameters.

Torsional ground motions also exist; however, since few if any actual recordings of torsional accelerations have been obtained, the true magnitude of this exciting force can only be estimated. Most researchers have neglected this phase of ground motion since past records would indicate translatory motions pose the greatest threat for structures.

The basic features of dynamic response such as frequency and mode shapes of some buildings, may be represented by a planar shear beam model. However, certain buildings with distinct centers of mass and rigidity have three-dimensional response and accordingly a three-dimensional shear beam model was developed by Hoerner [8]. This model has the ability to respond in rotation, to excitation which is purely translational. Response, therefore, may be significantly larger than would be expected from one-dimensional models.

Shephard [21] and others [10,11,19,23] have observed that strong coupling can occur when fundamental natural frequencies are close together. As a continuation of this work, a degree of coupling, represented in the mode shape of the model, is defined.

Other aspects which can influence fundamental frequency separation are the geometric layout of the building plan and the stiffness distribution. A study is presented, started by Newmark [17] which demonstrates the effect of plan and stiffness layouts with respect to frequency separation in systems which demonstrate two-fold symmetry, one-fold symmetry and asymmetric plan layout.

Current design procedures presented by the National Building Code [16], involve either a pseudo-static method, or a model spectrum analysis. These procedures are discussed in Chapter III and the treatment of torsional-translational

coupling is examined. A three-dimensional model, similar to that by Berg [2], is presented and variation of dynamic properties with respect to eccentricity is studied for the model.

The situation of period coincidence has been well discussed in detail by many researchers [10,11,21,23]. However, as is shown in Chapter IV, coincidence of real frequencies of dynamically unsymmetric systems is not possible. Period coincidence is therefore defined in terms of associated symmetric natural frequencies where coincidence can exist. With this definition, the validity of the spectrum technique is investigated over the range of period coincidence.

Shephard and Donald [2] proposed that the root mean square method of combining model response may underestimate the forces in a dynamically excited structure. Thus, an investigation is conducted to more fully understand this situation. A study is also presented, based on time history analysis and artificially generated earthquake records, to show the effect of period coincidence on dynamic response.

Conclusions obtained from the present investigations are presented in Chapter V. The effect of eccentricity and period coincidence can be significant and this implies that analysis more rigorous than presented in the Code is warranted in such cases.

CHAPTER II

IDEALIZED STRUCTURAL MODEL

CHAPTER II

IDEALIZED STRUCTURAL MODEL

2.1 INTRODUCTION

In this Chapter, the condition of dynamic assymmetry is studied, utilizing a simple model. Significant aspects of the dynamic properties are examined, showing the importance of closeness of frequencies to model coupling and the effect of geometric layout of a structure to its susceptibility to the coupling of translational and rotational motions. The effect of resistance layout to susceptibility to frequency coincidence in plans which exhibit two-fold symmetry, one-fold symmetry and assymmetry about principal axes is demonstrated.

2.2 DYNAMIC MODEL

The study of dynamic assymmetry utilizes a single mass model, developed by Hoerner [8]. This model is sufficiently representative of ~~real~~ structures, yet simple enough to distinguish recognizable patterns of behavior.

The single mass, three degrees of freedom system, shown in Fig. 2.1, is a structural representation of a single-storey building, with its mass located at floor-level. The model has assymmetric stiffness and three degrees of freedom- translation in the x and y directions and a rotation θ.

The equations of motion, considered about the center of mass, are

$$M\ddot{x} + (k_{x_1}+k_{x_2})(x-b\theta) + (k_{x_3}+k_{x_4})(x+b\theta) = 0$$

$$J\ddot{\theta} + b[(k_{x_3}+k_{x_4})(x+b\theta) - (k_{x_1}+k_{x_2})(x-b\theta)] +$$

$$a[(k_{y_1}+k_{y_4})(y+a\theta) - (k_{y_3}+k_{y_3})(y-a\theta)] = 0 \qquad (2.1)$$

$$M\ddot{y} + (k_{y_1}+k_{y_4})(y+a\theta) + (k_{y_2}+k_{y_3})(y-a\theta) = 0$$

where M represents the mass of the system, J the polar moment of inertia about the center of mass, k_x and k_y the individual column stiffness in the x and y direction, respectively.

The center of rigidity is defined by the relationship

$$(k_{x_1}+k_{x_2})(b-e_y) = (k_{x_3}+k_{x_4})(b+e_y)$$

$$(k_{y_1}+k_{y_4})(a-e_y) = (k_{y_2}+k_{y_3})(a+e_x) \qquad (2.2)$$

where e_x and e_y represent eccentricity in the x and y direction, respectively. In matrix form, these equations become

$$[M]\begin{Bmatrix}\ddot{x}\\ r\ddot{\theta}\\ \ddot{y}\end{Bmatrix}+\begin{bmatrix}K_x & -\frac{e_y}{r}K_x & 0\\ -\frac{e_y}{r}K_y & K_\theta & \frac{e_x}{r}K_y\\ 0 & \frac{e_x}{r}K_y & K_y\end{bmatrix}\begin{Bmatrix}x\\ r\theta\\ y\end{Bmatrix}=0 \quad (2.3)$$

where

$$K_x = \Sigma k_{xi} = k_{x_1} + k_{x_2} + k_{x_3} + k_{x_4}$$

$$K_y = \Sigma k_{yi} = k_{y_1} + k_{y_2} + k_{y_3} + k_{y_4}$$

$$K_\theta = \frac{1}{r^2}\Sigma(x_i^2 k_{yi}+y_i^2 k_{xi}) = \frac{1}{r^2}[a^2k_y+b^2k_x]$$

x_i, y_i represent the perpendicular distance to the resisting elements from the center of mass, and r the radius of gyration.

Expanding the simple model to N stories, it can be shown that similar equations apply. [8]

Since floors of most tall buildings have similar geometry, it can be assumed that their centroids lie in approximately the same position, so that it may be said they all lie on the same vertical line. [8] Accordingly, the polar radii of gyration would be the same. Adopting these conditions, the equations of motion, including viscous damping,

are given by

$$\begin{bmatrix} [M_1] & & 0 \\ & \ddots & \\ 0 & & [M_N] \end{bmatrix} \begin{Bmatrix} \ddot{x}_1 \\ \vdots \\ \ddot{x}_N \end{Bmatrix} + \begin{bmatrix} \left\{ \sum_{\substack{i=0 \\ j=1}}^{N} [C_{ij}] \right\} & \cdots & [C_{12}] & -[C_{1N}] \\ \vdots & & & \vdots \\ & & & -[C_{N-1,N}] \\ -[C_{1N}] & \cdots & [C_{N-1,N}] & \left\{ \sum_{\substack{i=1 \\ j=0}}^{N} [C_{Nj}] \right\} \end{bmatrix} \begin{Bmatrix} \dot{x}_1 \\ \vdots \\ \dot{x}_n \end{Bmatrix} +$$

$$\begin{bmatrix} [K_{01}] + [K_{12}] & -[K_{12}] & & 0 \\ -[K_{12}] & \left\{ [K_{12}] + [K_{23}] \right\} & & -[K_{N-1,N}] \\ & & \ddots & \\ 0 & & -[K_{N-1,N}] & [K_{n-1,N}] \end{bmatrix} \begin{Bmatrix} x_1 \\ \vdots \\ x_N \end{Bmatrix} = 0 \tag{2.4}$$

where $[M_i][C_{ij}]$ and $[K_{ij}]$ represent the following 3 x 3 mass, damping and stiffness matrices,

$$[M_i] = M_i \begin{bmatrix} 1 & & \\ & 1 & \\ & & \end{bmatrix} \tag{2.5}$$

$$[C_{ij}] = \begin{bmatrix} C_{x_{ij}} & -\delta_{y_i} C_{x_{ij}} & 0 \\ -\delta_{y_i} C_{x_{ij}} & C_{x_{ij}} & \delta_{x_i} C_{y_{ij}} \\ 0 & \delta_{x_i} C_{y_{ij}} & C_{y_{ij}} \end{bmatrix} \tag{2.6}$$

$$K_{ij} = \begin{bmatrix} k_{x_{ij}} & -\delta_{y_i} k_{x_{ij}} & 0 \\ -\delta_{y_i} k_{x_{ij}} & k\theta_{ij} & \delta_{x_i} k_{y_{ij}} \\ 0 & \delta_{x_i} k_{y_{ij}} & k_{y_{ij}} \end{bmatrix} \qquad (2.7)$$

The response vector, x_i is given by

$$x_i = \begin{Bmatrix} x_i \\ r\theta_i \\ y_i \end{Bmatrix} \qquad (2.8)$$

The terms δ_{x_i} and δ_{y_i} represent ratios of eccentricity to radius of gyration for the x and y direction, respectively, for the $i^{\underline{th}}$ level; $C_{x_{ij}}$ and $C_{y_{ij}}$ represent viscous damping in the x and y directions between the $i^{\underline{th}}$ and $j^{\underline{th}}$ floor levels; $k_{x_{ij}}$ and $k_{y_{ij}}$ represent interstorey stiffness between the $i^{\underline{th}}$ and $j^{\underline{th}}$ levels in the x and y directions, respectively.

2.3 EFFECT OF FREQUENCY COINCIDENCE ON COUPLING OF MOTION

For the simple system of Fig. 1, natural frequencies can be determined conveniently by transformation to generalized coordinates, utilizing

$$\begin{Bmatrix} q_1 \\ q_2 \\ q_3 \end{Bmatrix} = \begin{bmatrix} & I & \end{bmatrix} \begin{Bmatrix} x \\ r\theta \\ y \end{Bmatrix} \tag{2.9}$$

Generalized equations of motions become

$$[M]\{\ddot{q}\} + [K]\{q\} = 0 \tag{2.10}$$

Assuming a harmonic solution, in the form

$$\{\ddot{q}\} = -\omega_i^2 \{q\} \tag{2.11}$$

where ω_i represents the $i^{\underline{th}}$ natural circular frequency. Substitution yields

$$-\omega_i^2 [M]\{q\} + [K]\{q\} = 0 \tag{2.12}$$

Equation (2.12) represents the classical eigenvalue problem, where a non-trivial solution exists only if the associated determinant is zero. To reduce parameters, the model can be simplified by assuming symmetry about the x axis (i.e., $e_y = 0$).

Substituting $\omega_i^2 = \lambda_i$, the associated determinant becomes

$$\begin{bmatrix} k_x-\lambda_i M & & \\ & k_\theta-\lambda_i M & \delta k_y \\ & \delta k_y & k_y-\lambda_i M \end{bmatrix} = 0 \qquad (2.13)$$

where

$$\delta = \frac{e_x}{r} .$$

Solving the determinant, the solutions are

$$\omega_1^2 = \tfrac{1}{2}\left(\frac{k_\theta}{M} + \frac{k_y}{M} - \left(\left(\frac{k_\theta}{M} - \frac{k_y}{M}\right)^2 + 4\,\frac{k_y^2}{M^2}\,\delta^2\right)^{\frac{1}{2}}\right) \qquad (2.14)$$

$$\omega_2^2 = \frac{k_x}{M} \qquad (2.15)$$

$$\omega_3^2 = \tfrac{1}{2}\left(\frac{k_\theta}{M} + \frac{k_y}{M} + \left(\left(\frac{k_\theta}{M} - \frac{k_y}{M}\right)^2 + 4\,\frac{k_y^2}{M^2}\,\delta^2\right)^{\frac{1}{2}}\right) \qquad (2.16)$$

Equation (2.15) represents the uncoupled natural circular frequency in the x-direction.

The ratios $\left(\frac{k_\theta}{M}\right)^{\frac{1}{2}}$ and $\left(\frac{k_y}{M}\right)^{\frac{1}{2}}$ may be defined as the associated symmetric natural frequencies of the system indicated by ω'_θ and ω'_y respectively, calculated about the center of the mass.

The mode shapes of a system can demonstrate motion coupling. When centers of mass and rigidity are coincident, the rotational and translational responses are uncoupled and

independent. Upon introduction of eccentricity, each mode becomes coupled, containing both rotational and translational components. With this existence of coupling, a degree of coupling may be established defined as the contribution of another degree of freedom to the motion in the symmetrical uncoupled mode.

To obtain such an expression, the equation of motion [15] may be described as

$$[E^N]\ \{\phi_n\} = 0 \qquad (2.17)$$

where

$[E^N] = [k - \omega_n^2 M]$

$\{\phi_n\}$ = $n^{\underline{th}}$ mode shape of the system

ω_n = corresponding $n^{\underline{th}}$ natural circular frequency

The mode shapes of the system can be determined by solving for displacements in terms of one coordinate. Assuming a unit amplitude for the first element of the displacement vector,

$$\{\phi_n\} = \begin{Bmatrix} 1 \\ \phi_{1_n} \\ \phi_{2_n} \\ \vdots \\ \phi_{Nn} \end{Bmatrix} \qquad (2.18)$$

Substituting and expanding Eq. (2.17), utilizing matrix partitioning yields:

$$\left[\begin{array}{c|ccc} e_{11}^{N} & e_{12}^{N} & \cdots\cdots & e_{1N}^{N} \\ \hline e_{21}^{N} & e_{22}^{N} & & e_{2N}^{N} \\ e_{31}^{N} & e_{32}^{N} & & e_{3n}^{N} \\ \vdots & \vdots & & \vdots \\ e_{n1}^{N} & e_{N2}^{N} & & e_{Nn}^{N} \end{array}\right] \left\{\begin{array}{c} 1 \\ \phi_{2n} \\ \phi_{3n} \\ \vdots \\ \phi_{Nn} \end{array}\right\} = 0 \qquad (2.19)$$

For convenience, the above may be written symbolically as

$$\left[\begin{array}{c|c} e_{11}^{N} & E_{10}^{N} \\ \hline E_{01}^{N} & E_{00}^{N} \end{array}\right] \left\{\begin{array}{c} 1 \\ \phi_{0n} \end{array}\right\} = 0 \qquad (2.20)$$

After expansion, the following are obtained:

$$\begin{aligned} E_{01}^{N} + E_{00}^{N}\, \phi_{0N} &= 0 \\ e_{11}^{N} + E_{10}^{N}\, \phi_{0N} &= 0 \end{aligned} \qquad (2.21)$$

The displacement amplitudes may be derived by simultaneous solution of the equation.

$$\phi_{0N} = -\left(E_{00}^{N}\right)^{-1} E_{01}^{N} \qquad (2.22)$$

For the simple model, Eq. (2.22) becomes

$$\phi_{0N} = \frac{\delta k_y}{\omega_i^2 M - k_\theta} \tag{2.23}$$

Substituting the value for ω_i^2 yields

$$\phi_{0N} = \frac{\delta k_y}{M\left(\frac{1}{2}\left(\frac{k_\theta}{M} + \frac{k_y}{M} \pm \sqrt{\left(\frac{k_\theta}{M} - \frac{k_y}{M}\right)^2 + \frac{k_y}{M}\delta^2}\right)\right) - k_\theta} \tag{2.24}$$

Dividing by M and substituting the expressions for the associated symmetric natural frequencies (ASNF) yields

$$\phi_{0N} = \frac{2\delta\omega_y'^2}{(\omega_y'^2 - \omega_\theta'^2) \pm \sqrt{(\omega_\theta'^2 - \omega_y'^2)^2 + 4\delta^2\,\omega_y'^4}} \tag{2.25}$$

or

$$\phi_{0N} = \frac{2\delta}{1 - \left(\frac{\omega'_\theta}{\omega'_y}\right)^2 \pm \sqrt{\left\{\left(\frac{\omega'_\theta}{\omega'_y}\right)^2 - 1\right\}^2 + 4\delta^2}} \tag{2.26}$$

The mode shape for the system described is

$$\begin{Bmatrix} Y \\ r_\theta \end{Bmatrix} = \begin{Bmatrix} 1 \\ \dfrac{2\delta}{1 - (\dfrac{\omega'_\theta}{\omega'_Y})^2 \pm \left(\left(\dfrac{\omega'_\theta}{\omega'_Y}\right)^2 - 1\right)^2 - 4\delta^2)^{\frac{1}{2}}} \end{Bmatrix} \tag{2.27}$$

The expression

$$\frac{2\delta}{1 - (\dfrac{\omega'_\theta}{\omega'_Y})^2 \pm \left(\left(\dfrac{\omega'_\theta}{\omega'_Y}\right)^2 - 1\right)^2 - 4\delta^2)^{\frac{1}{2}}} \tag{2.28}$$

may be defined as the degree of coupling. It can be seen that if eccentricity is zero, no coupling exists, and upon the introduction of an eccentricity, coupling is introduced. This coupling is directly proportional to eccentricity and inversely proportional to the separation of associated symmetric natural frequencies.

The expression is dimensionless, and represents the degree of participation of another motion type to a symmetrical mode, and is designated by ψ.

The effect of frequency separation has added importance in the vicinity of coincidence, as noted by other researchers. [14,21,23] Referring to Fig. 2.2, the degree of coupling versus frequency ratio, it can be seen that severe coupling occurs in the range of frequency coincidence, being governed primarily by the value of eccentricity, as expected. The National Building Code [16] implies a frequency separation of less than ± 20% could give rise to sympathetic resonance. With regard to Fig. 2.2, this value would appear reasonable, for small eccentricities; however, for moderately large values of eccentricity, a ± 30% separation might be a more reasonable value.

It would also appear that the commencement of severe coupling is directly proportional to eccentricity, as well as frequency separation. Thus a single parameter such as frequency separation might not be sufficient to estimate the range of strong coupling for the probable values of eccentricity one may encounter.

2.4 EFFECT OF BUILDING PLAN ON MODAL COUPLING

The influence of frequency or period coincidence on modal coupling having been demonstrated, it is of interest to examine those aspects of a structure which give rise to this condition. Three basic structural parameters are involved:

(i) stiffness distribution

(ii) mass distribution

(iii) geometric plan layout

Although mass and stiffness distributions can relate directly to the geometric plan of a structure, for uniform distributions of mass, stiffness distribution and geometric layout become the principal parameters. The effect of these parameters on frequency ratios $\frac{\omega'_\theta}{\omega'_x}$ are now examined, this study having been done in part by Newmark. [17]

2.4.1 Rectangular Plan

For a rectangular plan, exhibiting two-fold symmetry, two possible cases of stiffness distribution are shown in Fig. 2.3.

For the uniformly distributed stiffness layout of Fig. 2.3(a), the rigidities in the x and y-directions are

$$K_x = k_x ab \tag{2.29}$$

$$K_y = k_y ab \tag{2.30}$$

where K_x, K_y represent the total stiffness and k_x, k_y represent the unit stiffness in the x and y-directions, respectively. Torsional rigidity is

$$K_\theta = K_y x^2 + K_x y^2 \tag{2.31}$$

where x and y are the perpendicular distances from the resisting elements to the center of the mass.

Substitution yields

$$K_\theta = \frac{ab}{12}(k_x a^2 + k_y b^2) \tag{2.32}$$

Since the centers of mass and rigidity coincide, the polar moment of inertia is

$$J = Mr^2 = \rho abr^2 \tag{2.33}$$

r being the radius of gyration, ρ, the mass density; and M, the total mass.

The associated symmetric natural frequencies ω'_x and ω'_θ are

$$\omega'_x = \left(\frac{k_x\, ab}{M}\right)^{\frac{1}{2}} \tag{2.34}$$

$$\omega'_\theta = \left(\frac{ab(k_x a^2 + k_y b^2)}{12Mr^2}\right)^{\frac{1}{2}}$$

With a uniformly distributed mass, the radius of gyration, r, is expressed as

$$r^2 = \frac{a^2 + b^2}{12} \tag{2.35}$$

Substituting and simplifying, the frequency ratio is

$$\frac{\omega'_\theta}{\omega'_x} = \left[\frac{k_x a^2 + k_y b^2}{k_x(a^2+b^2)}\right]^{\frac{1}{2}} \tag{2.36}$$

Referring to Fig. 2.4, it can be seen that for a stiffness ratio, $\frac{k_x}{k_y}$, is equal to 1, all aspect ratios a/b yield a frequency ratio equal to 1. For stiffness ratios different from 1, the curves appear to tend to unity with increasing aspect ratios. For the curves of Fig. 2.2, strong coupling can be expected as frequency ratio approaches unity, thus for this type of plan, with a stiffness ratio of one, strong coupling can be expected for any magnitude of eccentricity. For stiffness ratios different from 1, it would appear that the smaller the aspect ratio, the tendency to strong modal coupling may be diminished.

For the plan shown in Fig. 2.3(b), the stiffness is distributed uniformly along the perimeter. The translational stiffnesses are

$$K_x = 2a\ k_x$$

$$K_y = 2b\ k_y \tag{2.37}$$

The torsional stiffness is given by

$$K_\theta = \frac{ab^2 k_x + ba^2 k_y}{2} \tag{2.38}$$

The polar moment of inertia being the same as before, the associated symmetric natural frequencies become

$$\omega'_x = \left(\frac{2a\ k_x}{M}\right)^{\frac{1}{2}} \tag{2.39}$$

$$\omega'_\theta = \left(\frac{6ab(bk_x+ak_y)}{M(a^2+b^2)}\right)^{\frac{1}{2}} \tag{2.40}$$

Simplification yields

$$\frac{\omega'_\theta}{\omega'_x} = \left[\frac{3b(bk_x+ak_y)}{k_x(a^2+b^2)}\right]^{\frac{1}{2}} \tag{2.41}$$

The effects of aspect and stiffness ratios on frequency ratios are shown by the curves of Fig. 2.5. For stiffness ratios equal to one or less, the desired frequency separation is present for a wide range of aspect ratios. For stiffness ratios greater than one, aspect ratios less than 1.5 appear to yield the frequency separation desired by the code.

Reviewing the curves of Figs. 2.4 and 2.5, it is evident that rectangular layouts with peripheral stiffness

exhibit far less susceptibility to strong coupling in comparison to similar layouts with uniformly distributed stiffness. It may also be noted that the frequency separation desired by the code is present for moderately wide range of stiffness and aspect ratios, for rectangular layouts with peripheral stiffness; however, adequate frequency separation does not exist for similar plans with uniformly distributed stiffness.

2.4.2 T-Shaped Plan

Three examples of possible T-shaped plans are shown in Figure 2.6, covering two structural systems, that of uniformly distributed stiffness, (Fig. 2.6(a)), and that of peripheral stiffness (Figs. 2.6(b) and 2.6(c)).

For the plan of Fig. 6(a), with uniformly distributed stiffness and mass, centers of the mass and resistance coincide as the plan exhibits one-fold symmetry.

Translational stiffnesses are given by

$$K_x = \int_A k_x \, dA = 4ab \, k_x \tag{2.42}$$

$$K_y = \int_A k_y \, dA = 4ab \, k_y \tag{2.43}$$

where k_x, k_y are unit stiffnesses and dA denotes differential area. Mass is given by

$$M = 4\rho ab \tag{2.44}$$

The rotational stiffness, about the center of rigidity, is

$$K_\theta = \int_A (k_x y^2 + k_y x^2)\, dA \tag{2.45}$$

Integration yields

$$K_\theta = 2.167\ ab^3 k_y + 1.083 a^3 b\ k_x \tag{2.46}$$

The associated polar moment of inertia is

$$J = (2.33b^2 + 1.083a^2)\rho ab \tag{2.47}$$

The associated natural frequencies

$$\omega'_x = \left(\frac{k_x}{\rho}\right)^{\frac{1}{2}} \tag{2.48}$$

$$\omega'_\theta = \frac{2.167\ b\ k_y + 1.083\ a^2 k_x}{\rho(2.33\ b^2 + 1.083\ a^2)} \tag{2.49}$$

yield the frequency ratio

$$\frac{\omega'_\theta}{\omega'_x} = \left[\frac{1.083\ a^2\ k_x + 2.167\ b^2\ h_y}{k_x(2.33\ b^2 + 1.083\ a^2)}\right]^{\frac{1}{2}} \tag{2.50}$$

The curves of Fig. 2.7 demonstrate the effects of the aspect ratio on the frequency ratio for various stiffness ratios. It may be noted that the stiffness ratios different

from 1, in the range of aspect ratios less than 1, yield less susceptibility to strong coupling and provide the code frequency separation. Generally, this particular layout and stiffness distribution lead to strong coupling over a wide range of aspect and stiffness ratios. A similar plan, with peripheral stiffness, as shown in Fig. 2.6(b) has translational stiffnesses

$$K_x = 2\ k_x$$

$$K_y = 2\ k_y \tag{2.51}$$

and rotational stiffness, about the center of the mass

$$K_\theta = 1.125\ a^2 k_x + 4.5\ b^2\ k_y \tag{2.52}$$

With the expression for mass and polar moment of inertia given by Eqs. (2.44) and (2.47) the resulting frequency ratio is

$$\frac{\omega'_\theta}{\omega'_x} = \left[\frac{1.125\ a^2\ k_x + 4.5\ b^2\ k_y}{k_x(4.66\ b^2 + 2.166\ a^2)}\right]^{\frac{1}{2}} \tag{2.53}$$

The curves of Fig. 2.8, give the variation of frequency ratio with respect to aspect and stiffness ratios for the above expression. Again, for stiffness ratios different from 1, and aspect ratios less than 1, this particular layout of plan and stiffness exhibit diminished susceptibility to strong coupling.

For most aspect ratios, moderate susceptibility to strong coupling is expected, however less pronounced than with uniformly distributed stiffness. For the stiffness layout shown in Fig. 2.6(c), basically similar to that of Fig. 2.6(b), but with increased eccentric peripheral stiffness, the frequency ratio is

$$\frac{\omega'_\theta}{\omega'_x} = \left[\frac{2.25(b^2 k_y + a^2 k_x)}{2.33\, b^2 + 1.083\, a^2) k_x}\right]^{\frac{1}{2}} \qquad (2.54)$$

Setting the aspect ratio equal to unity and the stiffness ratio to 2, the frequency ratio yields 0.994. This would imply that strong coupling is expected.

It is evident that a T-shaped plan lends itself to strong modal coupling under a large variety of stiffness distributions, over a wide range of stiffness and aspect ratios.

2.4.3 L-Shape Plan

The last plan considered, asymmetrical about its principal axes, is the L-shaped plan, shown in Fig. 2.9. The plans shown have both uniformly distributed stiffness and peripheral stiffness.

For the uniformly distributed mass, the translational stiffnesses are

$$K_x = 3\ ab\ k_x$$
$$K_y = 3\ ab\ k_y \qquad (2.55)$$

The rotational stiffness is given by

$$K_\theta = 0.9166\ k_y\ a^3 b + 0.9166\ k_x\ ab^3 \qquad (2.56)$$

The mass and polar moments of inertia are

$$M = 3\ ab\ \rho \qquad (2.57)$$

and

$$J = \rho\ ab(0.9166\ a^2 + 0.9166\ b^2) \qquad (2.58)$$

Combining and simplifying the frequency ratio becomes

$$\frac{\omega'_\theta}{\omega'_x} = \left[\frac{a^2\ k_y + b^2\ k_x}{k_x(a^2+b^2)}\right]^{\frac{1}{2}} \qquad (2.59)$$

Examining the curves of Fig. 2.10, the plot of frequency ratio with respect to aspect ratio, shows that for stiffness ratios different from 1 and aspect ratios greater than 1.5, the desired frequency separation implied by the code is obtained,and there exists less tendency to strong coupling. For aspect ratios less than 1.5, and particularly for a stiffness ratio of 1, strong coupling would be expected.

Considering the same plan, with possible peripheral stiffness arrangement, as shown in Fig. 2.9(b), the rotational stiffness is

$$K_\theta = 2.055\ (a^2\ k_y + b^2\ k_x) \qquad (2.60)$$

The frequency ratio is

$$\frac{\omega'_\theta}{\omega'_x} = 1.860 \left[\frac{(a^2 k_x + b^2 k_y)}{k_x (a^2+b^2)}\right]^{\frac{1}{2}} \qquad (2.61)$$

The curves of Fig. 2.11 show that for all aspect and stiffness ratios plotted, there appears no tendencies towards strong coupling and the desired frequency separation sought by the code is obtained.

2.4.4 Summary

From this study of geometric plans and stiffness distributions, it is noted that structures which have uniformly distributed stiffness, exhibit associated symmetric natural frequency ratios close, if not equal to, one. This situation implies the possibility of strong coupling and may be encountered with closely spaced columns and flat slab construction. Geometric layouts with peripheral stiffness concentrations exhibit greater frequency separation, implying decreased susceptability to strong coupling. Thus, even in instances with systems where the eccentricity is minimal, strong coupling may occur because of the plan and stiffness layout.

CHAPTER III

NATIONAL BUILDING CODE'S PROVISIONS CONCERNING TORSION

CHAPTER III

NATIONAL BUILDING CODE'S PROVISIONS CONCERNING TORSION

3.1 INTRODUCTION

The purpose of this chapter is to review current National Building Code provisions relating to torsion. Code philosophy for aseismic design and its treatment of torsional effects is discussed. Both the recommended static and dynamic methods are reviewed. The effects of variation of eccentricity on dynamic properties of the structural model are discussed. The effects of eccentricity according to the Code static and Dynamic methods are presented.

3.2 CODE PHILOSOPHY

Performance criteria implicit in the code are that structures should resist major catastrophic earthquakes without collapse, moderate earthquakes with minor structural damage and minor seismic disturbance without damage. Collapse state is defined as failure of the primary structure where occupant escape is not possible.

Inhabitant safety is the prime concern and accordingly factors which complicate a structure's response to dynamic excitation must be considered. It can be shown that a structure under excitation has a finite amount of energy to dissipate. Asymmetry does not appreciably affect the total

energy received by a structure [9]. The magnitude of the maximum stress, however, is affected by asymmetry, [20] resulting in concentrated energy dissipation in certain resisting elements.

3.3 NBC TREATMENT OF TORSION

The 1975 National Building Code of Canada (NBC) [16] provides two procedures for seismic design force determination; one, a static method, based on dynamic considerations, the other, model spectrum analysis. Both guidelines have provisions to account for theoretical and accidental eccentricities, amplification caused by closeness of torsional and translational frequencies, effects of dynamic magnification of torsional moments and the effect of simultaneous action of two horizontal components of ground motion.

3.3.1 Static Method

The static method as described in "Commentary J", provides guidelines for a static approach to seismic design forces.

Total lateral seismic force is calculated from

$$V = A\ S\ K\ I\ F\ W \qquad (3.1)$$

where

V = total lateral seismic force

A = horizontal design ground acceleration

S = seismic coefficient

K = a factor to account for various structural systems

I = importance factor

F = foundation factor

W = weight of structure

The lateral seismic force, F_x, is distributed to each level, x, by

$$F_t = (V-F_c) \frac{w_x h_x}{\left(\sum_{i=1}^{N} w_i h_i \right)} \qquad (3.2)$$

where

w_x, w_i = portion of W located at level "x" or "i" respectively

h_x, h_i = height to level "x" or "i" respectively

F_t = portion of V concentrated at the top of a structure to account for "whip lash"

Torsional effects result from theoretical and accidental eccentricities. Accidental eccentricity is account for by an eccentricity consideration equivalent to 5% of the plan dimension in the direction of motion being considered.

Theoretical and accidental eccentricity are combined by

$$e_D = 1.5\ e + 0.05\ D_N$$

or (3.3)

$$0.5\ e + 0.05\ D_N$$

where

e_D = design eccentricity

e = theoretical eccentricity

D_N = plan dimension in direction under consideration

The governing case being the one which results in the largest member stress.

Increasing or decreasing the theoretical eccentricity by 50% accounts for dynamic magnification and the simultaneous action of two horizontal ground motion components.

Torsional moments in the horizontal plane for each storey, are

$$M_{ti} = (V - \sum_{i=1}^{i} F_x) e_{Di} \qquad (3.4)$$

where

M_{ti} = torsional moment for level i

F_x = lateral seismic force at level x

e_{Di} = design eccentricity for level i

However, when design eccentricity exceeds 50% of plan dimension;

(a) a dynamic analysis is mandatory, or

(b) results of Eq.(3.4) are doubled.

Closeness of frequencies is noted, from which large torsional amplifications can occur, however, a procedure to identify such cases is not given.

3.2.2 Spectrum Analysis

The guidelines outlined in Commentary "K" [16], inertia forces of a structure and the corresponding dynamic response are determined utilizing normal modes of the structure. An average design spectrum is provided, as reproduced in Fig. 3.1.

Dynamic force contributions for mode j and storey level i, are calculated by

$$P_{ij} = \phi_{ij} \cdot \gamma_j \cdot s_{nj} \cdot m_i \qquad (3.5)$$

where

P_{ij} = lateral storey force for level i and mode j

ϕ_{ij} = normal mode component for mode j at level i

γ_j = modal participation factor for mode j

S_{aj} = elastic spectral acceleration for mode j having period T

m_i = mass assigned to level i

Torsional effects are computed either by:

(a) uncoupled analysis

(b) coupled analysis

Uncoupled analysis assumed lateral modes de-coupled along the two principal axes and may only be used when theoretical eccentricity is less than $0.05\ D_N$ in all stories and a minimum ± 20 percent separation exists between fundamental torsional and lateral frequencies. Design eccentricity is calculated from Eq. (3.3). Torsional moments M_i at any level i are

$$M_i = P_i . e_D \tag{3.6}$$

and total torsional moments in storey $i = k$ are

$$M_k = \sum_{i=N}^{k} M_i \tag{3.7}$$

If frequency separation does not exceed ± 20%, torsional moments are doubled to account for possible sympathetic resonance.

Coupled analysis, the consideration that torsion and translational modes are coupled, utilizes rotational and translational degrees of freedom in the eigenvalue formulation.

This analysis is used when the theoretical eccentricity exceeds 0.10 D_N. To account for accidental eccentricities and torsional ground motions, the torsional moments throughout the structure are increased or decreased by 25 percent, whichever produces the worst effect in a member. Either uncoupled or coupled analysis may be used when the maximum theoretical eccentricity lies between 0.05 D_N and 0.10 D_N.

3.4 STRUCTURAL MODEL

For purposes of analysis, a structural model is presented, as shown in Fig.3.2. The model previously proposed by Berg [2] as a plane frame is expanded to a 3-dimensional multi-degree of freedom system. The structural representation retains original member stiffnesses in the plane of each frame. The out-of-plane stiffness of each column corresponds to the in-plane stiffness of the column of the intersecting perpendicular frame, thus rendering each frame in either direction equal. The model is symmetric in plan, about the two principal axes, x and y.

For analysis, certain simplifying assumptions are made. Floor slabs are considered rigid in their own plane, this having been verified by experiment [18]. A mass of the structure is considered to be concentrated at floor levels, creating a discrete model. The motion of the structure, at each level, is represented by the motion of the center of each mass. Vertical motions and non-linear be-

haviour are neglected. These assumptions are consistent and have been employed by a number of other researchers [8,13].

For the purpose of this study, the eccentricity e, shown in Fig. 3.2, is created by shifting the center of the mass an equal amount at each level. The eccentricity is unidirectional and the percent eccentricity is defined as the ratio e/D, D being plan dimension in the x direction.

Thus, the model is established as dynamically unsymmetrical, having a single eccentricity in the x-direction, which remains constant through the course of the subsequent study. However, for the investigation discussed in Chapter IV, the eccentricity is created by modifying the stiffness of exterior frames in the y-direction, the center of mass being coincident with the center of plan. Equal alterations to the frame stiffnesses in the x-direction produce the varying degrees of period coincidence described, as indicated by the ratio of torsional-to-translational frequencies.

The direction of the excitation is the y-direction, for all investigations.

3.4.1 Dynamic Properties

The model exhibits the following dynamic properties:

(a) period variation with eccentricity

(b) modal variation with eccentricity

(c) primarily translational coupled modes

(d) primarily torsional coupled modes

Figure 3.3 demonstrates fundamental period variation as a function of eccentricity ratio, e/D. The primarily translational period increases with eccentricity while the primarily torsional period decreases, trends evident from examination of Eqs. (2.14) through (2.16).

Considering the concept of contribution factors [20] and using expansion theory, it can be shown that any vector ϕ representing the motion of a system in eigenvalue space can be expressed as a linear combination of the uncoupled natural symmetric modes of the system.

$$\phi = C_1\phi^{(1)} + C_2\phi^{(2)} + C_3\phi^{(3)} + \ldots + C_j\phi^{(j)} + C_N\phi^{(N)} \tag{3.8}$$

where ϕ is any coupled modes shape and $\phi^{(1)}$ is the $j^{\underline{th}}$ uncoupled natural symmetric mode of the system. Premultiplying by $\underline{\phi}^{(j)T}\,\underline{M}$, where $\underline{M}$ is the mass matrix,

$$\underline{\phi}^{(j)T}\,\underline{M}\,\underline{\phi} = C_j\,\underline{\phi}^{(j)T}\,\underline{M}\,\underline{\phi}^{(j)} \tag{3.9}$$

and using orthogonality of modes

$$C_j = \frac{\underline{\phi}^{(j)T}\,\underline{M}\,\underline{\phi}}{\underline{\phi}^{(j)T}\,\underline{M}\,\underline{\phi}^{(j)}} \tag{3.10}$$

where C_j represents the contribution of the $j^{\underline{th}}$ uncoupled natural symmetric mode to vector ϕ. By calculating the value of C_j the contribution of the uncoupled natural symmetric modes to the coupled modes can be seen as shown in Figures 3.4 and 3.5.

Contribution of the uncoupled symmetric translational mode to the primarily translational mode of the coupled system and its variation with increasing eccentricity is shown in Fig. 3.4. Contribution of the uncoupled symmetric torsional mode to the primarily torsional mode is shown in Fig. 3.5.

The contribution of the uncoupled translational mode decreases with increasing eccentricity while the coupled torsional motion becomes more pronounced with increasing eccentricity. The rate of increase of a second motion type appears most pronounced in the small to moderate range of eccentricity, (0 to 20%).

Contribution of uncoupled symmetric translational motion to the coupled mode appears constant above a value of ≈ 25% eccentricity. It would appear that additional eccentricity, beyond 25% produces no marked changes in the mode shapes of the coupled system.

Examining Fig. 3.5 which shows contributions of the symmetric mode shapes to the primarily torsional mode, con-

clusions similar to those noted above may be drawn.

The range of small-to-moderate eccentricity (0 to 20%) produces the most rapid rate of change of the mode shape. Accordingly, it may be concluded that an increase or decrease of eccentricity in this range has greater effect in altering dynamic properties of the model than in the range of large eccentricity.

3.5 EFFECT OF ECCENTRICITY BY CODE STATIC METHOD

The torsional effects on the model are now examined for an eccentricity range of 0 to 25%, according to the Code of Static Method [16].

Total lateral seismic force is calculated from Eq. (3.1) for an assumed horizontal ground acceleration of 10% G, G being the acceleration due to gravity.

Seismic coefficient S and period T are 0.678 and 0.4 seconds respectively. The K factor, for a ductile space frame is 0.7 and all other factors are assumed equal to unity.

The total lateral seismic force V is 99^{k}. Storey torsional moments, calculated from Eq. (3.4), are distributed as follows. [23]

The total rotational stiffness K_{θ}, about the center

of rigidity is

$$K_\theta = \Sigma(k_y x^2 + k_x y^2) \qquad (3.11)$$

k_x, k_y = lateral frame stiffness in x and y direction

x, y = perpendicular distance from the frame line to center of rigidity

Torsional frame shear V_t is

$$V_t = \frac{M_T \times K}{K_\theta} \qquad (3.12)$$

M_T = torsional moment

K = total stiffness of frame-line under consideration

x = perpendicular distance from the frame-line to center of rigidity

The increase in top floor displacement and frame base shear subject to combined torsional and translational motions is shown in Figs. 3.6 and 3.7. The diagrams represent the additive effect of the two motion types.

The percentage increase over uncoupled motion, for the same parameters, is shown in Figs. 3.8 and 3.9. Accidental eccentricity, represented by zero theoretical eccentricity, increases base shear by 9% and 3% for external

and internal frames respectively. The distribution of torsional shears is directly proportional to the distance from the resisting element to the center of rigidity, as shown by Figs. 3.8 and 3.9 and by Eq. (3.12). The increase in base shear or displacement is linear since code provisions, in the static procedure, merely add shear to account for torsional effects. Simultaneous action effects of two horizontal ground motions and dynamic magnification are accounted for only by the design eccentricity, e/D.

3.6 EFFECT OF ECCENTRICITY BY CODE SPECTRUM METHOD

Utilizing dynamic analysis procedures, design seismic forces are now calculated for the structural model. Coupled analysis is used in conjunction with the NBC average design spectrum, shown in Fig. 3.1.

As stated previously, design ground acceleration of 10% G is assumed. Ductility factor of 4, representative of ductile space frames, and 5% viscous damping are also assumed. In an attempt to include stiff and flexible structures, two models with corresponding symmetric natural periods in translation of 0.5 and 2.0 seconds respectively, are studied. The computer program TABS [27] is used to calculate structural responses. Table 3.1 lists the periods of structures used, over the range of eccentricities encountered. No torsional magnificated is included, as coupl-

ed analysis involves this phenomenon directly.

3.6.1 Stiff Building

The plots of structural response for a stiff building defined as having a symmetric translational period approximately equal to 0.5 sec are shown in Figs. 3.10 and 3.11. Response parameters presented are frame base shear and top floor displacement. Each frame, having the same lateral stiffness renders the two series of curves similar and are discussed simultaneously.

The behavior of Figs. 3.10 and 3.11 may be explained by three distinct factors, acting concurrently:

(i) modal coupling of torsional and translational motions

(ii) period lengthening with increasing eccentricity

(iii) movement of center of mass, origin for the equations of motion

Coupling effect increases with eccentricity, as noted in Figs. 3.10 and 3.11. Thus, all frames in the y-direction exhibit response based on combined effects of two distinct motion types. Response of frames in the x-direction is due to the effect of coupling only.

With increasing eccentricity, there is translational period lengthening, seen in Fig. 3.3. Examining Fig.3.1,

the NBC average design spectrum, it can be shown that increasing translational period decreases spectral acceleration.

In TABS, the equation of motion is written about the center of mass. As mentioned previously, the eccentricity is produced by offsetting the center of mass with respect to the center of rigidity, to produce the desired eccentricity. With increasing eccentricity, distances from each frame line vary, resulting in different distributions of torsional shears.

The response plot of frame 8 increases with eccentricity up to approximately 15% eccentricity after which the decreasing in distance from the center of mass plus the effect of period lengthening appear to counteract the coupling effect. The response plot of frame 5, basically the difference of motion types, decrease continually, due to effect of period lengthening and increased distance between frame line and center of mass.

Response plots of frames 6 and 7, (interior frames), show similar, though less pronounced behavior. The behavior of frame 7 demonstrates the effect of origin location, as after 17% eccentricity, the torsional motion no longer adds to translational responses but instead reduces it. This, combined with lengthening period, causes the observed reduction of response.

The response plot of frame 4 is due to coupling action alone, and the effect of lengthening period is evident also.

3.6.2 Flexible Building

The response plots of the flexible model, defined as having a symmetrical fundamental period of approximately 2.0 seconds, are shown in Figs. 3.12 and 3.13. Response parameters are frame base shear and top floor displacement.

From these curves, the same general observations apply as for the rigid structure.

CHAPTER IV

EXAMINATION OF PERIOD COINCIDENCE AND COUPLED SYSTEMS

CHAPTER IV

EXAMINATION OF PERIOD COINCIDENCE AND COUPLED SYSTEMS

4.1 INTRODUCTION

The purpose of this chapter is to investigate the concept and effects of period coincidence. The concept of period coincidence, with respect to actual period of the structure, is examined and a reasonable approximation is proposed. The validity of the modal spectrum analysis technique for coupled systems is studied by comparing modal spectrum response with response obtained from time history analysis.

4.2 CONCEPT OF PERIOD COINCIDENCE

The introduction of an eccentricity to a dynamically symmetrical system causes fundamental changes to that system's behavior, as translational and torsional motions become coupled and the fundamental periods of both motion types are altered, as previously noted in Chapters II and III.

Period coincidence, defined as the situation when one of the fundamental translational periods and the fundamental torsional periods are coincidence, does not exist in terms of dynamic systems with real eccentricities.

Recalling the characteristic equation of the simple dynamic model presented in Chapter II, the solution to Eq. (2.15) is

$$\omega^2 = \tfrac{1}{2}\left[\left(\frac{K_\theta}{M} + \frac{K_y}{M}\right) \pm \sqrt{\left(\frac{K_\theta}{M} - \frac{K_y}{M}\right)^2 + 4\frac{K_y^2}{M^2}\delta^2}\,\right] \quad (4.1)$$

where ω represents the natural frequency of the coupled translational or torsional mode. To obtain identical frequencies of the two motion types, and real period coincidence, repeated eigenvalues are sought. Eliminating trivial solutions repeated eigenvalues require that

$$\sqrt{\left(\frac{K_\theta}{M} - \frac{K_y}{M}\right)^2 + 4\frac{K_y}{M^2}\delta^2} = 0$$

Simplifying this means that for period coincidence

$$(K_\theta - K_y)^2 = -4K_y^2\delta^2 \quad (4.2)$$

In a physical sense, the difference between torsional and translational stiffnesses cannot be an imaginary number, rendering true period coincidence, in dynamically unsymmetrical systems, an impossibility. However, period coincidence can exist in terms of associated natural symmetric frequencies and it is using this concept that the following is presented.

Table 4.1 shows the associated natural symmetric

frequency ratios as well as the actual frequency ratios. It would appear that after 20% separation in the associated natural symmetric frequencies, the ratios of these frequencies gives acceptably accurate predictions of the real frequency ratios.

4.3 VALIDITY OF MODAL SPECTRUM ANALYSIS IN COUPLED SYSTEMS

In coupled three-dimensional systems, as in two-dimensional systems, when using modal spectrum analysis techniques, the total structural response is usually obtained by combining individual modal response with the root mean square (RMS) method. The validity of this approach [21] is questionable in a situation of period coincidence or near period coincidence. The RMS method relies on the modes having significantly different periods implying that maximum response occurs at different times. However, in situations of near period coincidence, it may arise that maximum response of the two modes occurs at approximately the same time. Accordingly, total response tends to be an algebraic sum of the two modal responses, as has been shown by previous research [21,23].

To examine this point, 3 psuedo earthquakes records were generated, using the program PSEQSN, [21] all statistically equal. The general characteristics of the artificially generated records are:

(a) peak acceleration of 10% G

(b) negligible build-up and decay times of 0.01 sec

(c) digitization at 0.01 sec intervals

(d) 10-second length of record

A value of 0.6 as the fraction of critical damping and a period of 0.4 sec were used for filter characteristics. These values tend to simulate records on firm ground and were obtained from a previous study on artificially generated earthquake records. [26]

From the records, acceleration spectrums for 2% damping were calculated.

Using the generated earthquake records, the time history response [27] of the model, described in Chapter III, was obtained for a variation of frequency ratios $\frac{\omega_\theta}{\omega_t}$ between 1 to 0.5 for ~~a~~symmetrical translational periods of 0.4 sec and 2.0 sec. The acceleration and velocity spectra are shown in Figs. 4.1 to 4.6.

Figure 4.7 shows the comparison of response spectrum techniques to time history analysis, with respect to period coincidence, for a rigid structure, corresponding to a symmetric translational period of 0.4 sec. It can be seen that the RMS method yields an underestimation of response. In comparison with two-dimensional systems, where only one motion type is evaluated, the RMS method is generally with-

in 5% of time history response [20]. It would appear that for rigid structures, a frequency separation of 30% is required to obtain a similar accuracy.

Figure 4.8 shows the comparison of RMS method to time history response for a flexible structure, corresponding to one with a dynamically symmetric translational period of 2.0 sec.

It would appear that frequency ratio does not significantly effect the RMS response for flexible structures, as viewed in Fig. 4.8.

The NBC implies a separation of ± 20% of the fundamental frequencies after which the designer need no longer account for sympathetic resonance. Based on the results shown in Figs.4.7 and 4.8.this separation would appear satisfactory for flexible structures, however, not sufficient for rigid structures. For rigid structures, a period separation in the order of 30% would correspond to a more acceptable degree of accuracy.

4.4 EFFECT OF PERIOD COINCIDENCE ON MAGNITUDE OF RESPONSE OF COUPLED SYSTEMS

The effects near coincidence of periods defined in terms of associated natural symmetric frequencies, are now investigated, utilizing the response parameters of frame base shear, top floor displacement and shear distribution.

The associated symmetries frequency ratios, with corresponding actual ratios, and the coupled torsional and translational periods are listed in Table 4.2. For the translational periods shown, and referring to the acceleration spectrum of Figs.4.1 to 4.3, it is evident that as frequency separation increases, there is a corresponding decrease in translational period, resulting in an increased value for the associated spectral acceleration.

As noted previously, assymmetry does not appreciably affect the total energy received by a structure, but does affect the distribution or magnitude of maximum stress [26]. This is seen in the response of the exterior frames in the y-direction, shown in Fig.4.9. As coincidence is approached, a redistribution of shears occurs, diminishing rapidly as separation increases. Frame 8, being stiffer than frame 5, due to the manner in which the eccentricity was varied, attracts significant amounts of shear. Eccentricity is created by adjusting the stiffness of the exterior frames in the y-direction to shift the center of resistance, in the positive y-direction, to produce the desired separation between centers of mass and resistance. The increase in base shear, for ratios less than 0.9, is attributed to higher spectral acceleration and diminished coupling effects. Also, it may be noted that as separation increases, the average of all frame base shears in the y-direction, increases continuously.

The response of interior frames in the y-direction is shown in Fig.4.10. Similar behavior patterns, although less pronounced, are evident in the range of $\frac{\omega'_\theta}{\omega'_T} > 0.9$. In the range of $\frac{\omega'_\theta}{\omega'_T} < 0.9$, diminishing coincidence effects and higher spectral accelerations govern frame response.

The response of frames in the x-direction is due to coupling and defines the degree of coupling introduced in the total response. Top floor displacement is used to demonstrate this effect in Fig. 4.11.

Normalized shear distribution, is shown in Fig.4.12. It is apparently not significantly affected by period separation.

CHAPTER V

SUMMARY AND CONCLUSIONS

CHAPTER V

SUMMARY AND CONCLUSIONS

Previous studies by other researchers have shown that the dynamic behavior of structural systems can be predicted, in part, by discrete models.

The results in this study are limited to ideally elastic behavior. The equations of motion for a lumped mass, 3-degrees of freedom system, were examined in Chapter II. Attention was directed to the effect of frequency coincidence on the coupling motion with an attempt to establish a degree of coupling. The behavior of this parameter was investigated over a range of frequency ratios and degrees of eccentricity and it is found that strong coupling is related to both eccentricity and frequency separation.

The effect of geometric layout and distribution of stiffness, was investigated with respect to period coincidence for plans with uniformly distributed mass. Rectangular layouts, simulating two-fold symmetry, were found to have high sensitivity towards period coincidence for uniformly distributed stiffness over a large range of aspect and translational stiffness ratios. Rectangular layouts, with peripheral stiffness show far less sensitivity to period coincidence over the same range of aspect and translational stiffness ratios.

T-shape layouts, having one-fold symmetry, were shown to have moderate-to-high susceptibility to period coincidence for both uniformity distributed and peripheral stiffness layouts.

L-shape layouts, simulating asymmetry about the principal axes, are shown to exhibit moderate susceptibility for uniformly distributed stiffness and no susceptibility for peripheral stiffness layouts.

It was noted that for layouts studied, uniformly distributed stiffness, similar to that of a flat slab, closely spaced columns type of construction shows a high susceptibility to period coincidence and thus should be regarded with caution as the potential for strong coupling is present.

In Chapter III, the National Building Code philosophy was briefly discussed and recommended procedures for both dynamic and static analysis for seismic induced loadings were reviewed. A structural model, was used to investigate the effect of eccentricity on dynamic behavior, based on code procedures. The effect of eccentricity and the dynamic properties was shown. The behavior of a flexible and rigid structure, with increasing eccentricity, was investigated. The effect of eccentricity was found to increase most rapidly in the range of moderate eccentricity (< 20%), beyond which the effect of increasing eccentricity does not significantly change the response.

The examination of the effect of period coincidence on coupled systems was presented in Chapter IV. The concept of period coincidence was defined to exist only in terms of associated natural symmetric frequencies and not in terms of real frequency of coupled systems. The validity of modal spectrum analysis was investigated in the context of period coincidence. It was found that the root mean square (RMS) method of combining modal response underestimates the total response in situations of period coincidence or near coincidence. The error was found to be significant for rigid structures, less for flexible ones. It was noted that this method does not appear suitable in the frequency range of $1 \leq \frac{\omega_\theta}{\omega_T} \leq 0.8$.

The effect of period coincidence was examined for a coupled system with a fixed eccentricity using a time history analysis. The dynamic behavior was noted over a range of frequency ratios and a redistribution of base shears among frames was found to exist in the vicinity of $\frac{\omega_\theta}{\omega_T} = 1.0$. This redistribution is found to be significant for the exterior frames, less so for interior frames.

It can be concluded from this study that the effects of eccentricity in conjunction with small separation of torsional and translational frequencies can be significant. Based on the results of the study of modal spectrum techniques with respect to coincidence, it can be concluded that period coincidence or near coincidence requires a more rigorous time history analysis to obtain the total response

to acceptable accuracy.

REFERENCES

REFERENCES

[1] Ayre, R.S., "Interconnection of Translational and Torsional Vibrations in Buildings," Bulletin of Seismological Society of America, Vol. 28, (1938).

[2] Berg, G.V., "The Analysis of Structural Response to Earthquake Forces", Ph.D. Thesis, University of Michigan, (1958).

[3] Blume, J.A., Newmark, N., and Corning, L.H., "Design of Reinforced Concrete Building for Earthquake Motions," Portland Cement Association, (1961).

[4] Blundy, D., "The Plywood Palace", Sunday Times, London, England, (January 25, 1975).

[5] Clough, R.W., and Penzion,J., Dynamics of Structures, McGraw-Hill, N.Y. (1975).

[6] Esteva, L., Rascon, O.A., and Gutierey, A., "Lessons From Some Recent Earthquakes in Latin America," Proceedings 4th World Conference on Earthquake Engineering, Vol.3, Santiago, Chile, (1969), pp.58-73.

[7] Hart, G.C., DiJulio, R.M., and Lew, M., "Torsional Response of High-Rise Buildings," J. Struct.Div., ASCE, Vol. 101, No.ST2, (Feb.1975),pp.397-416.

[8] Hoerner, J., "Modal Coupling and Earthquake Response of Tall Buildings," Ph.D.Thesis, California Institute of Technology, Pasadena, California, (1971).

[9] Housner,G.W., and Outiner, H., "The Effect of Torsional Oscillations on Earthquake Stresses", Bulletin Seimological Society of America, Vol.48, (July 1958), pp.221-229.

[10] Kan, L., and Chopra, A., "Effects of Torsional Coupling on Earthquake Forces in Buildings," J. Struct. Div., ASCE, Vol.103,ST4, (April 1977), pp.805-819.

[11] Kan, L., and Chopra, A., "Elastic Earthquake Analysis of a Class of Torsionally Coupled Buildings," J.Struct. Div., ASCE, Vol.103, ST4, (April 1977), pp.821-838.

[12] Keintzel, E., "On the Seismic Analysis of Unsymmetrical Storied Buildings," Proc. 5th World Conference on Earthquake Engineering, Rome, Italy, (1973), pp.110-113.

[13] Koh, T., Takase, H., and Tsugawa, T., "Torsional Problems in Seismic Design of High-Rise Buildings," Proc. 4th World Conference on Earthquake Engineering, Santiago, Chile, (1969).

[14] Mazilu, P., Sandi, H., Teodorescu, D., "Analysis of Torsional Oscillations," Proc. 5th World Conference on Earthquake Engineering, Rome, Italy, Vol. 2, (1973), pp.153-162.

[15] Medearis, K., "Coupled Bending and Torsional Oscillations of a Modern Skyscraper," Bulletin Seimological Society of America, Vol. 56/4, (Aug.1966), pp.938-950.

[16] Anonymous, National Building Code of Canada, (1975).

[17] Newmark, M.N., "Torsion in Symmetrical Buildings," Proc. 4th World Conference on Earthquake Engineering, Santiago, Chile, Vol. 3, (1969), pp.19-32.

[18] Nielsen, N.N., "Dynamic Response of Multistorey Buildings", Ph.D.Thesis, California Institute of Technology, Pasadena, California, (June, 1964).

[19] Penzion,J., "Earthquake Response of Irregularly Shaped Buildings," Proc. 4th World Conference on Earthquake Engineering, Santiago, Chili, (1969).

[20] Roesset, J.M., Fundamentals of Earthquake Engineering for Buildings, Massachusetts Institute of Technology, (1972).

[21] Ruiz, P., and Penzien, J., PSEQGN, Artificial Generation of Earthquake Accelerograms, University of California, California, (1969).

[22] Shepard, H., and Donald,R.N., "Seismic Response of Torsionally Unbalanced Buildings," J. Sound and Vibration, Vol.6, (January 1967), pp.20-37.

[23] Skinner, R.I., Skilton,D.W.C., and Laws, D.A., "Unbalanced Buildings and Buildings With Light Towers Under Earthquake Forces," Proc. 3rd World Conference on Earthquake Engineering, Vol.2, Auckland and Wellington, New Zealand, (1965).

[24] Tso, W.K., "Induced Torsional Oscillations in Symmetric Structures," J. Earthquake Engineering and Structural Dynamics, Vol.3, (1975).

[25] Tso, W.K., Asmis,K.C., "Torsional Vibrations of Symmetrical Structures," 1st Canadian Conference on Earthquake Engineering, Vol.1, Vancouver, Canada, (1971).

[26] Tso, W.K., Guru, B.B., "A Statistical Study on Artificially Generated Earthquake Records," 2nd Canadian Conference on Earthquake Engineering, McMaster University, Hamilton, Ontario, (1975).

[27] Wilson, E.L., Dovey, H.H., "Three-Dimensional Analysis of Building Systems TABS," Earthquake Engineering Research Center Report, No. EERC 78-8, (1972).

TABLES

TABLE 1 PERIODS FOR THE STRUCTURES USED FOR NBC DYNAMIC METHOD

% ECC	T_{TRANS} (SEC)		T_{TORS} (SEC)		$\frac{\omega_\theta}{\omega_T}$
	Rigid	Flex	Rigid	Flex	
0 (uncoupled)	0.50	2.0	0.387	1.549	.774
5	0.5054	2.0216	0.3831	1.532	.758
10	0.5198	2.079	0.3725	1.49	.7167
15	0.54	2.160	0.3585	1.434	.664
20	0.564	2.256	0.3433	1.373	.6086
25	0.5905	2.362	0.328	1.312	.555
30	0.6189	2.4758	0.3128	1.251	.5053
35	0.649	2.5961	0.298	1.193	.4595

TABLE 2 FREQUENCY RATIOS AND COUPLED PERIODS FOR THE DYNAMIC MODEL

SYMMETRICAL SYSTEM			COUPLED SYSTEM		
FREQ. RATIO ω'_θ/ω'_T	TORSIONAL PERIOD T_θ (SEC)	TRANS. PERIOD T_y (SEC)	FREQ. RATIO ω_θ/ω_T	TORSIONAL PERIOD T_θ (SEC)	TRANS. PERIOD T_y (SEC)
1	0.40	.40	.905	.381	.421
0.95	0.38	.40	.898	.370	.412
0.90	0.36	.40	.869	.354	.407
0.85	0.34	.40	.834	.337	.404
0.80	0.32	.40	.789	.318	.403
0.70	0.28	.40	.694	.279	.402
0.60	0.24	.40	.596	.239	.401
0.50	0.20	.40	.499	.1998	.400

DRAWINGS

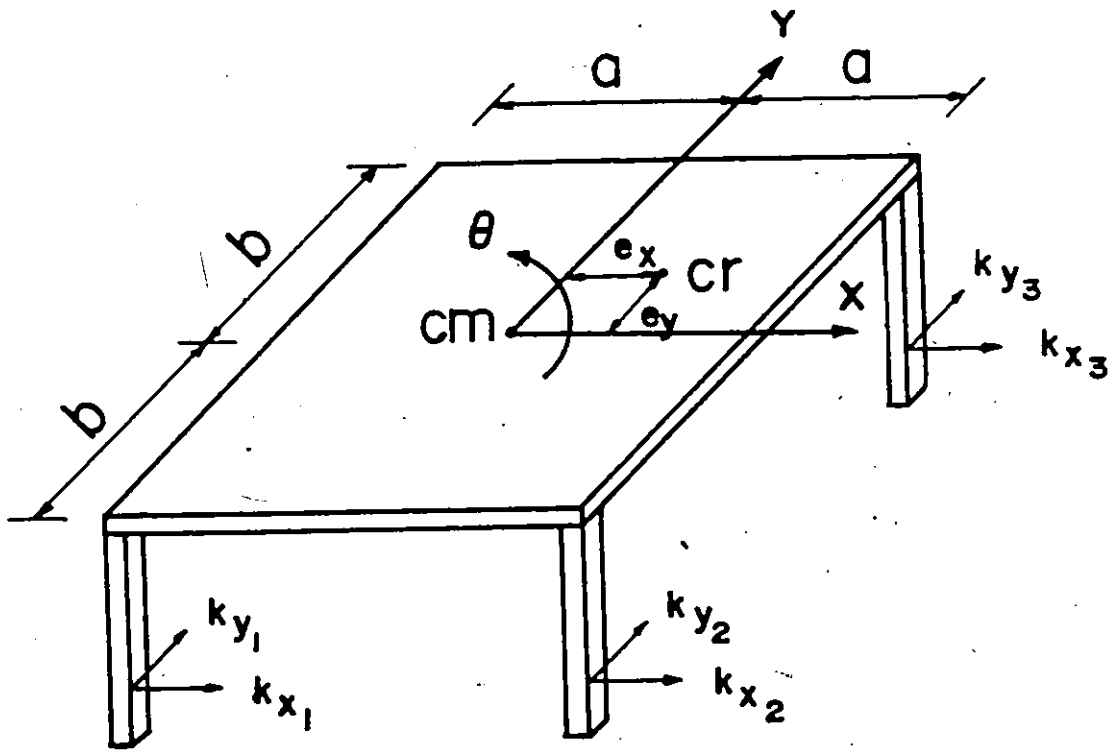

FIG. 2.1 DYNAMIC MODEL OF A STRUCTURE WITH ASSYMMETRIC STIFFNESS (single mass, three degrees of freedom system)

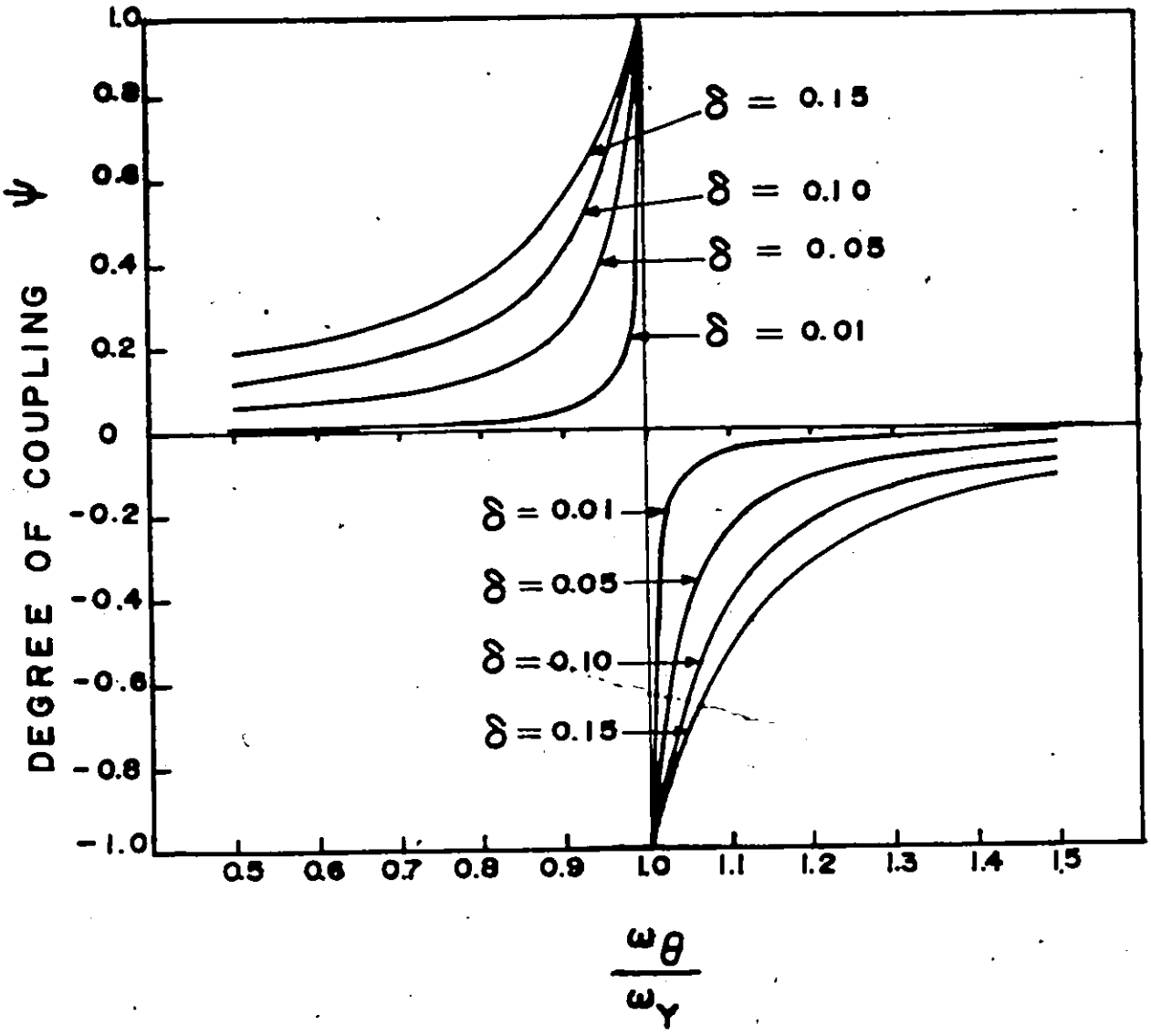

FIG. 2.2 DEGREE OF COUPLING versus FREQUENCY RATIO

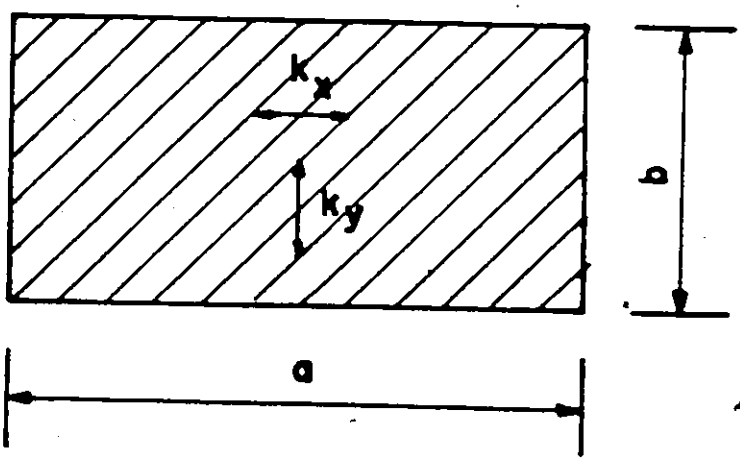

(A) UNIFORMLY DISTRIBUTED STIFFNESS

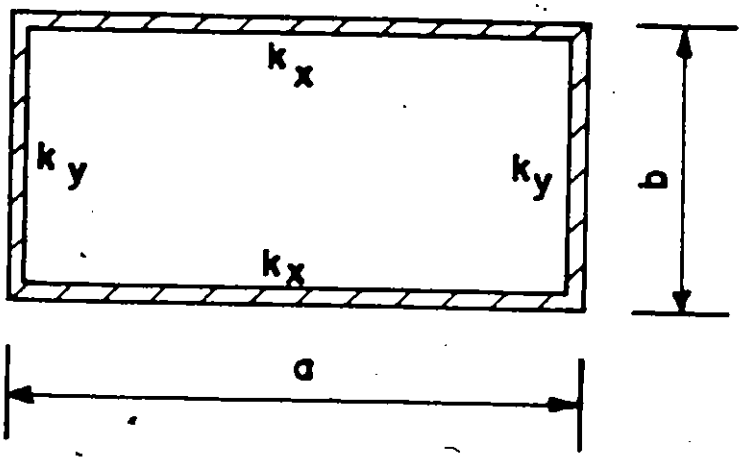

(B) STIFFNESS AROUND PERIMETER

FIG. 2.3 RECTANGULAR BUILDING PLAN

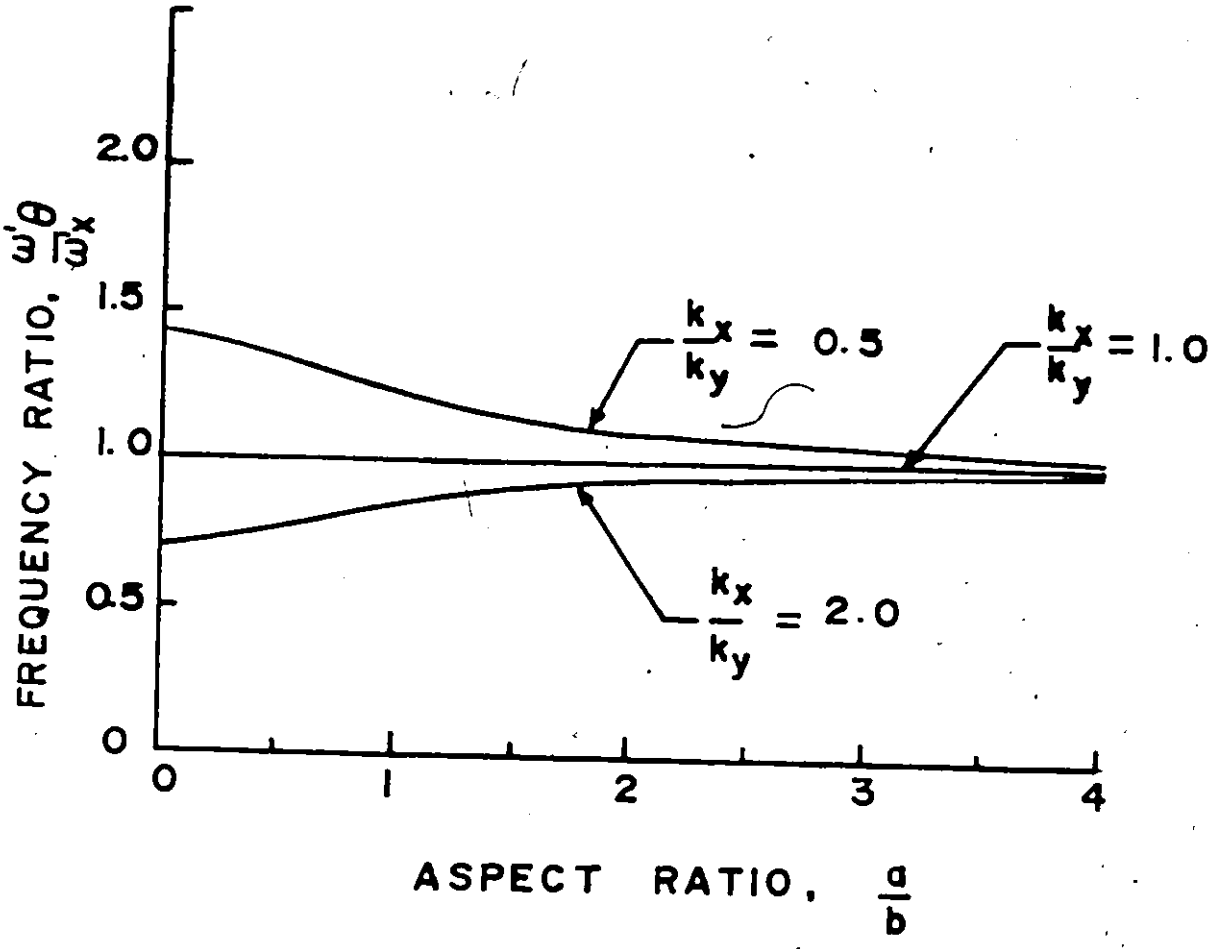

FIG. 2.4 FREQUENCY RATIO versus ASPECT RATIO- RECTANGULAR PLAN WITH UNIFORMLY DISTRIBUTED STIFFNESS

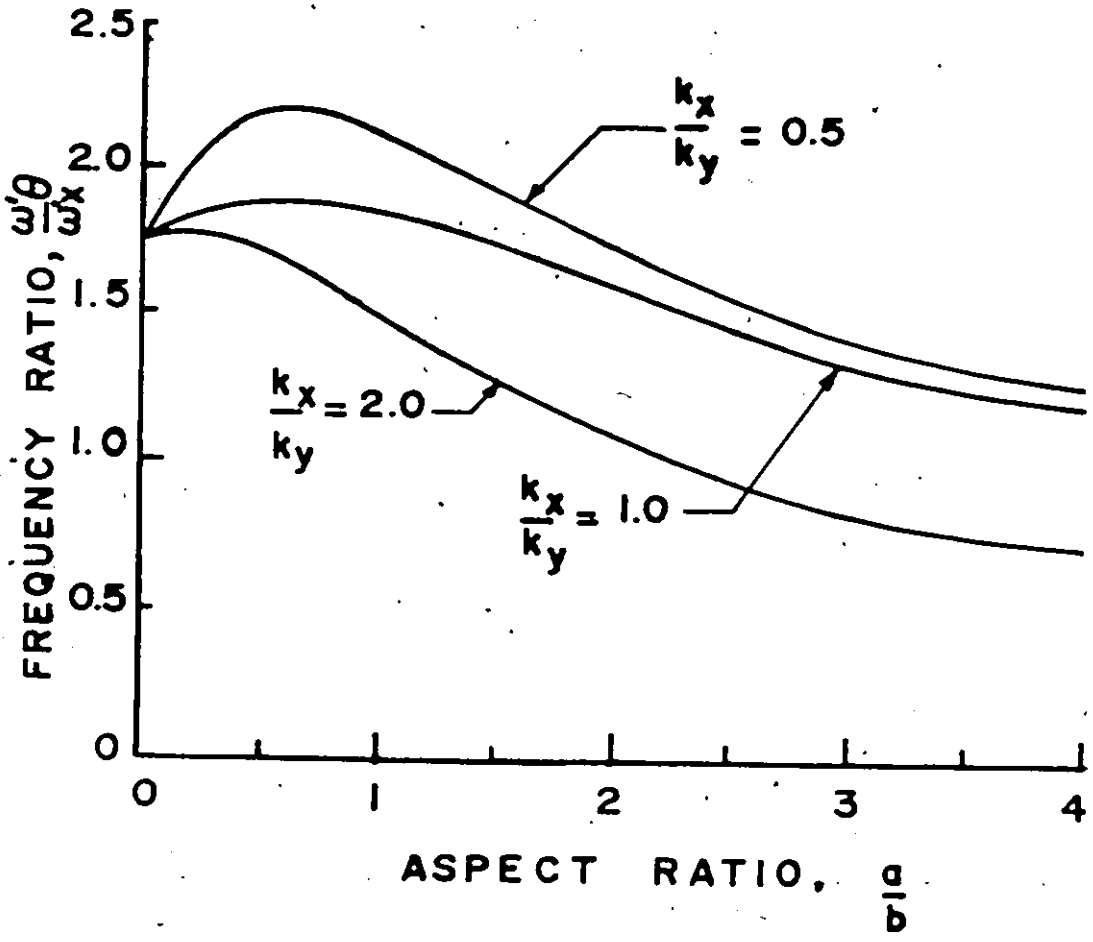

FIG. 2.5 FREQUENCY RATIO versus ASPECT RATIO-
RECTANGULAR PLAN WITH PERIPHERAL STIFFNESS

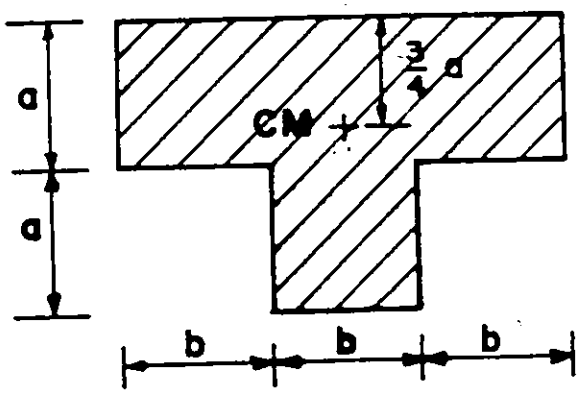

(a) UNIFORMLY DISTRIBUTED STIFFNESS

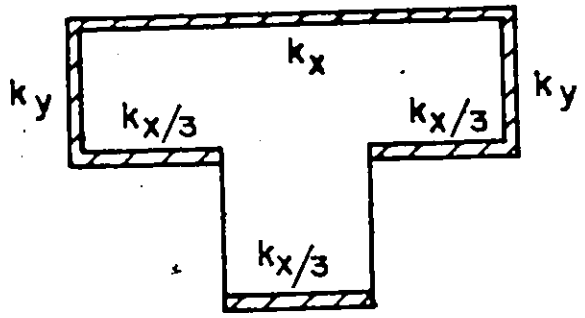

(b) PHERIPHERAL STIFFNESS

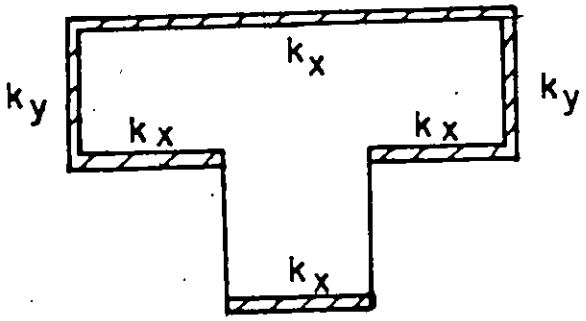

(c) PHERIPHERAL STIFFNESS

FIG. 2.6 T-SHAPED BUILDING PLAN

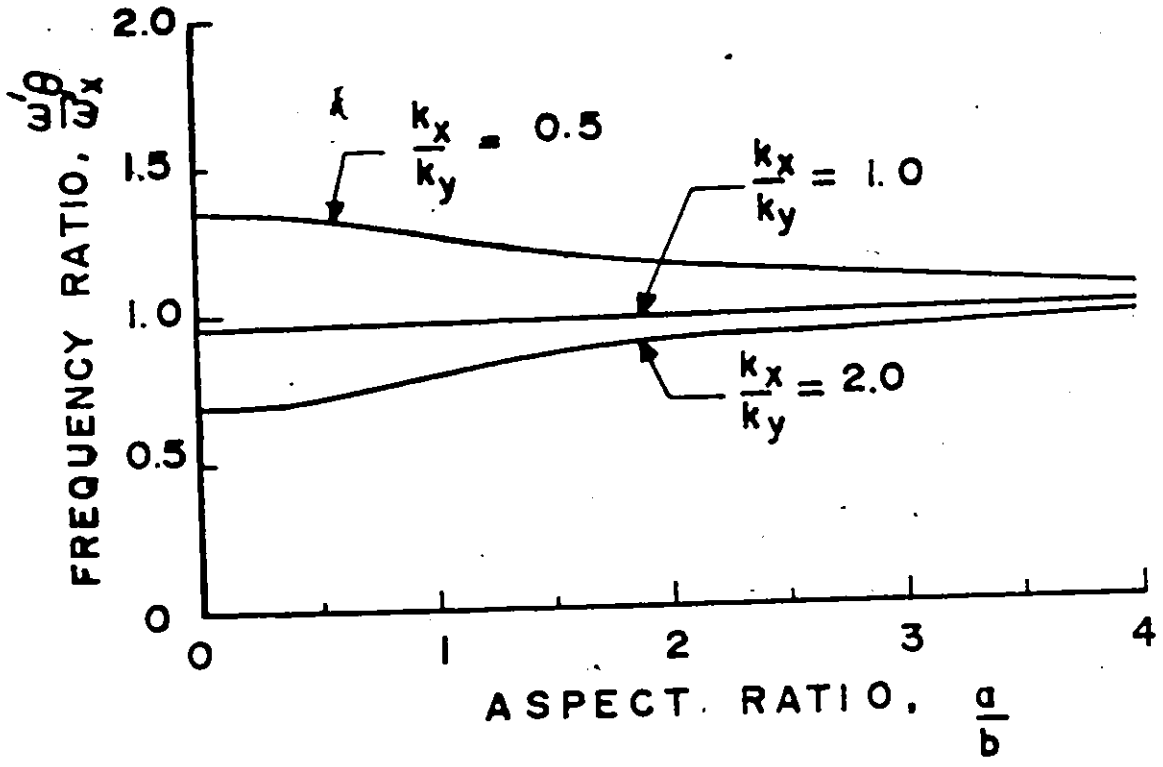

FIG. 2.7 FREQUENCY RATIO versus ASPECT RATIO-T-SHAPED PLAN WITH UNIFORMLY DISTRIBUTED STIFFNESS

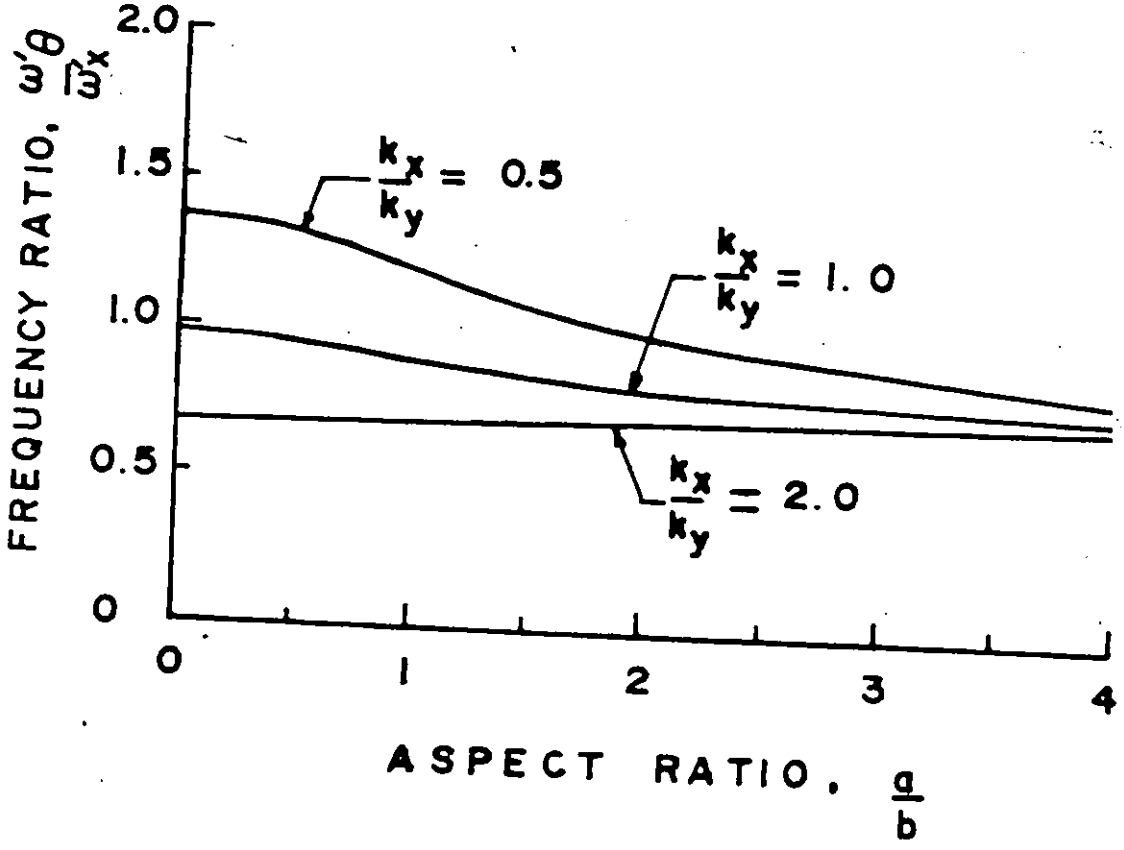

FIG. 2.8 FREQUENCY RATIO versus ASPECT RATIO-T-SHAPED PLAN WITH PERIPHERAL STIFFNESS

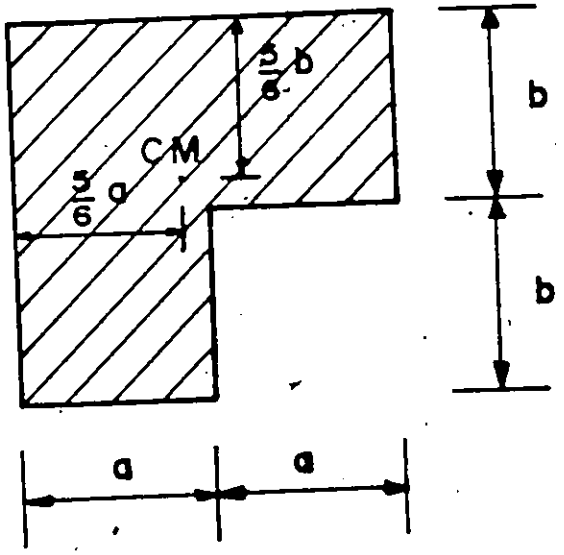

(a) UNIFORMLY DISTRIBUTED STIFFNESS

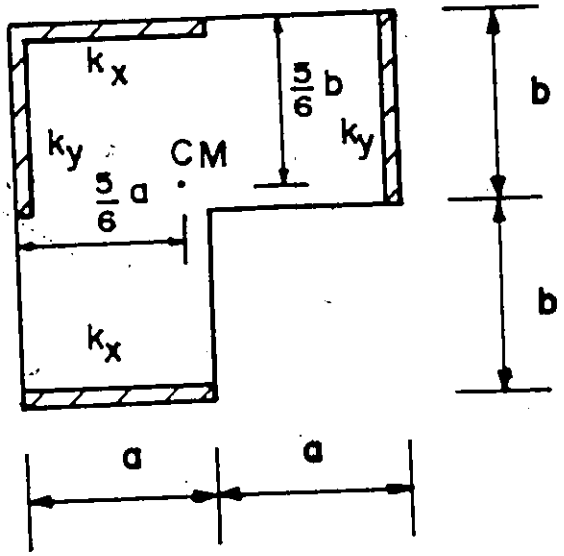

(b) PERIPHERAL STIFFNESS

FIG. 2.9 L-SHAPED BUILDING PLAN

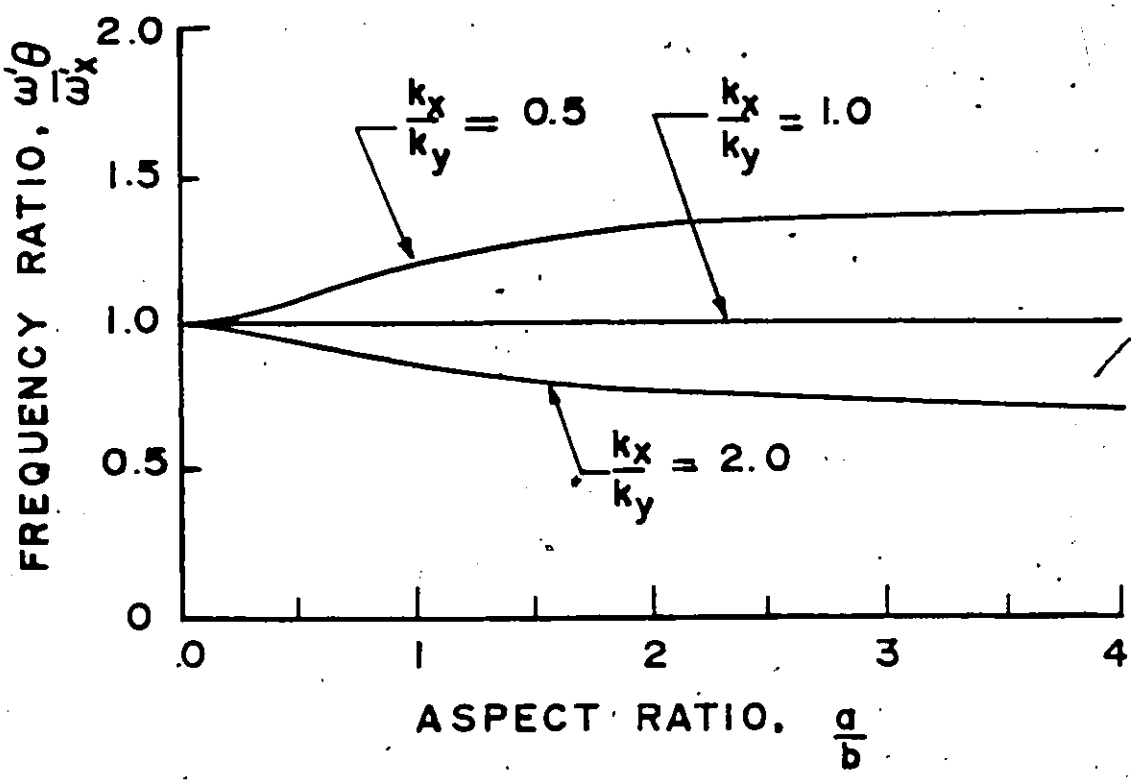

FIG. 2.10 FREQUENCY RATIO versus ASPECT RATIO-L-SHAPED PLAN WITH UNIFORMLY DISTRIBUTED STIFFNESS

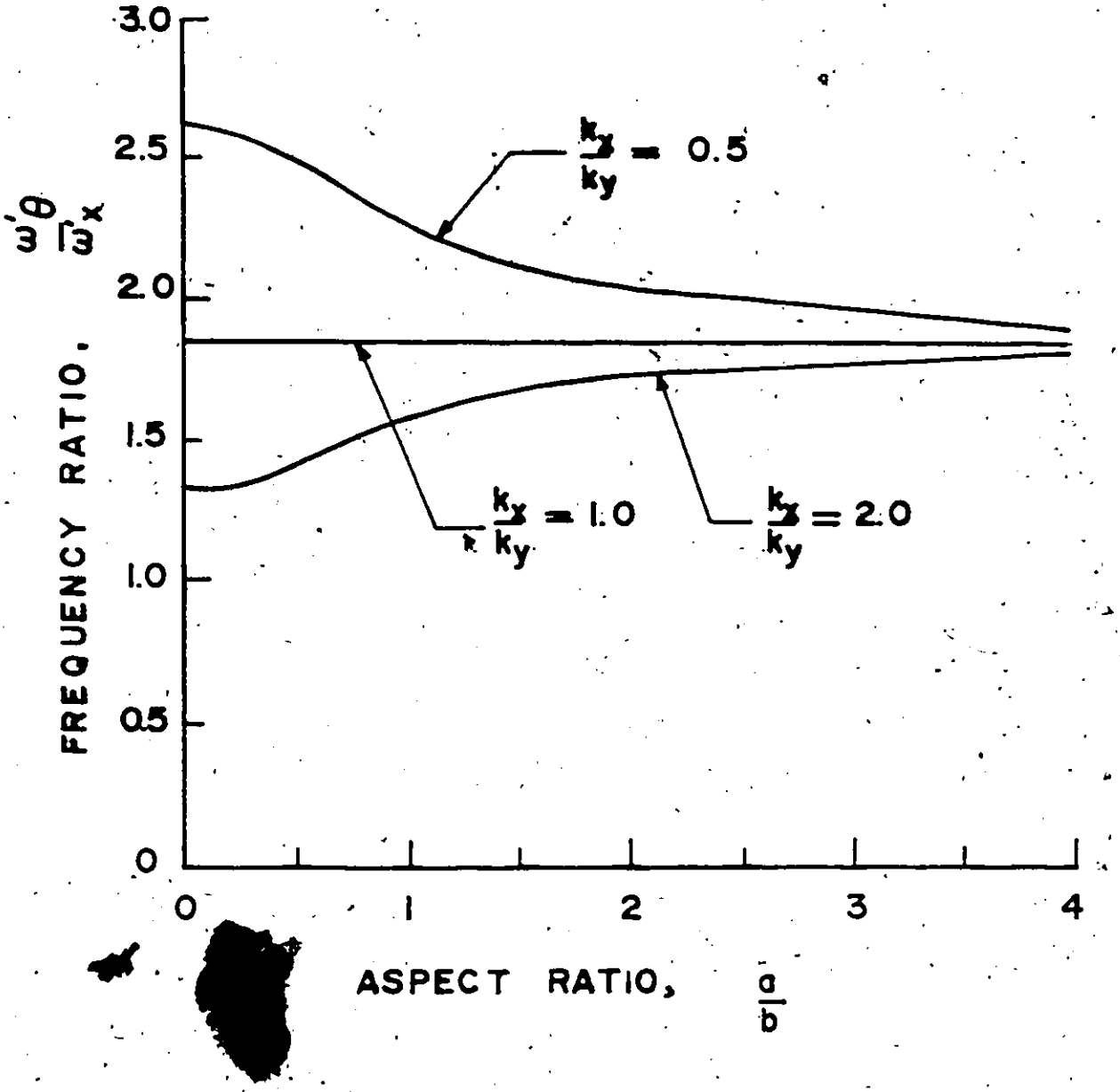

FIG. 2.11 FREQUENCY RATIO versus ASPECT RATIO-L-SHAPED PLAN WITH PERIPHERAL STIFFNESS

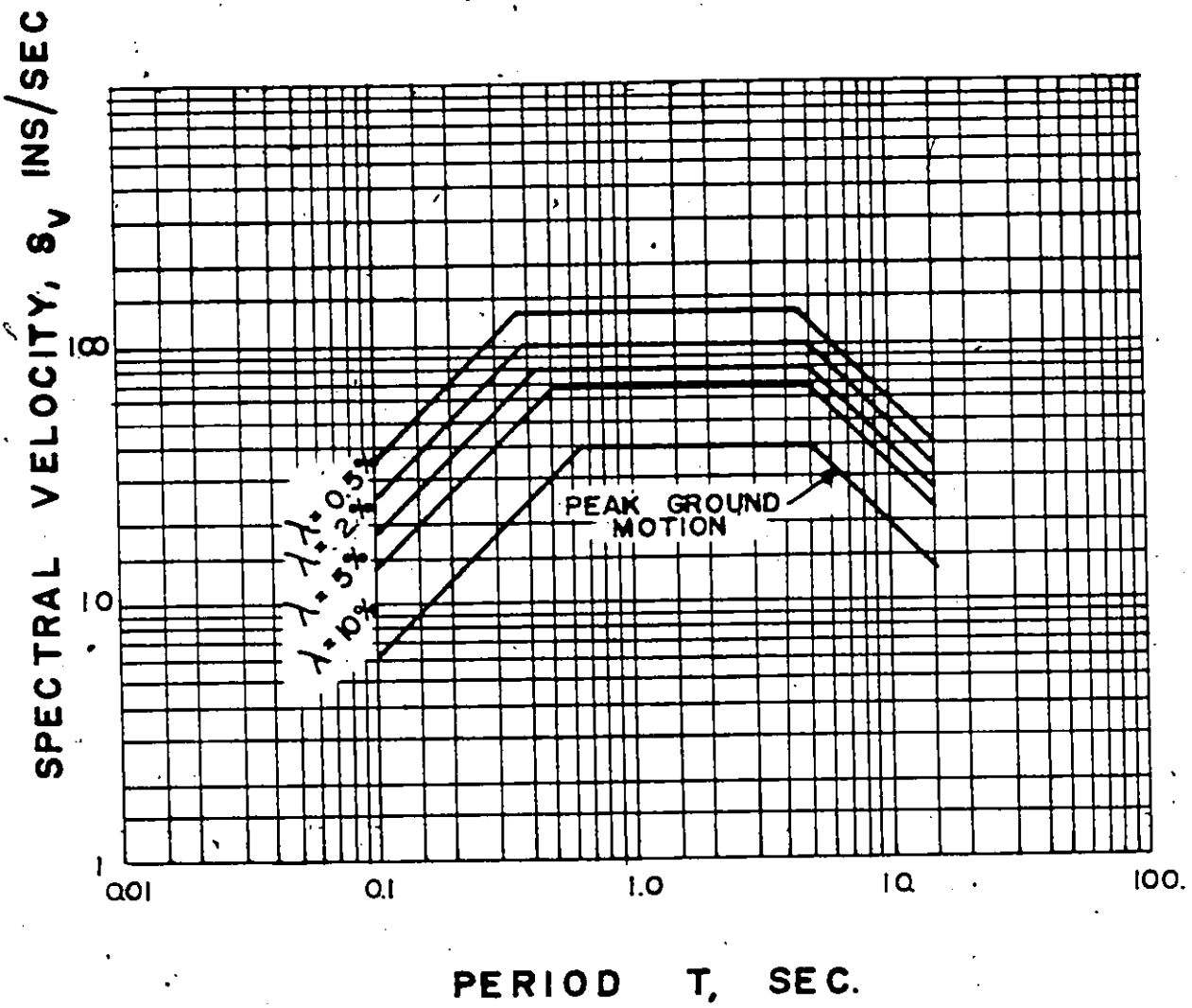

FIG. 3.1 NATIONAL BUILDING CODE AVERAGE DESIGN SPECTRUM. [6]

(Peak ground motion bounds and elastic average response spectrum for 1.0 G maximum ground acceleration)

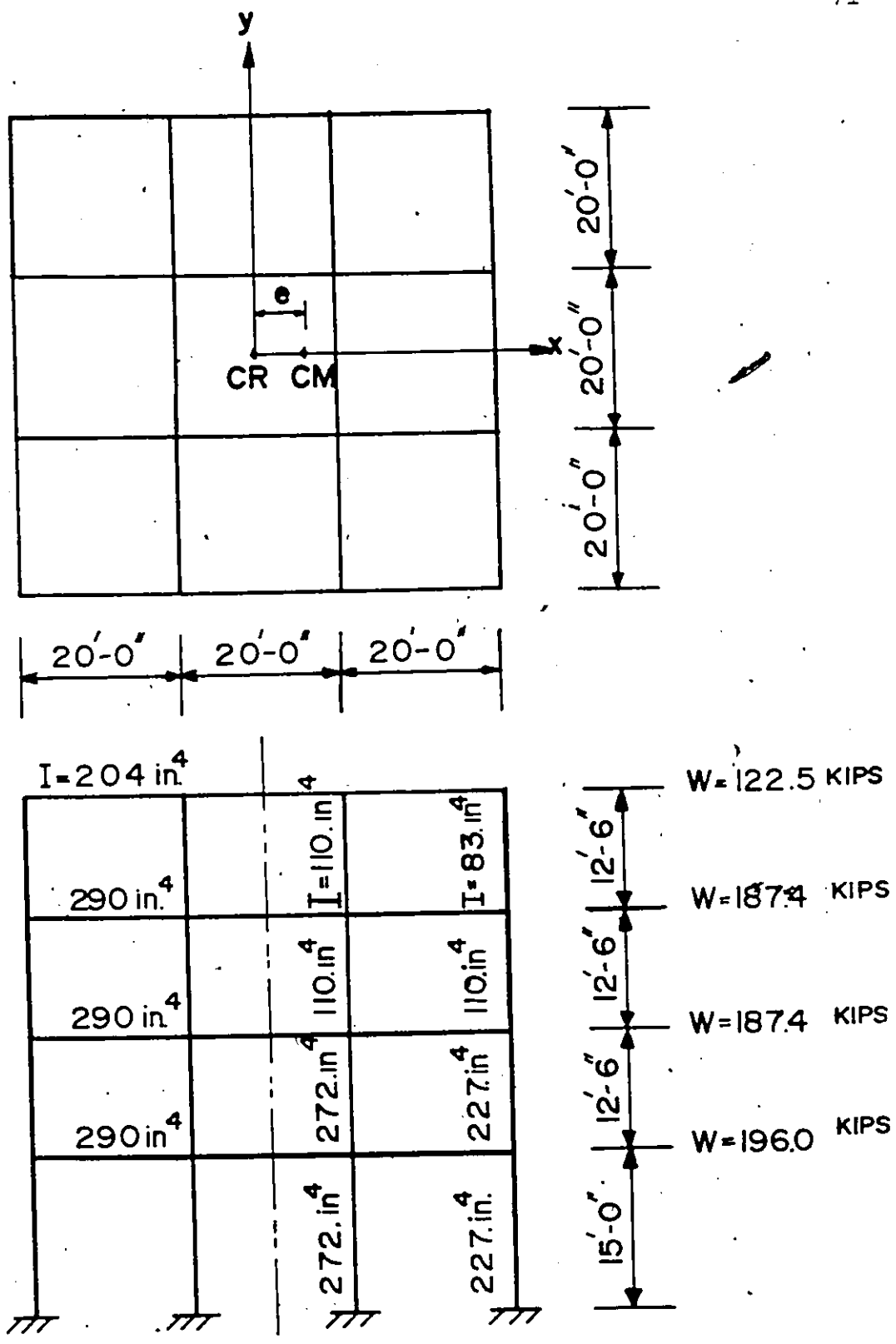

FIG. 3.2 MODEL OF 3-DIMENSIONAL FRAMED STRUCTURE

(Multi-degree of freedom.)

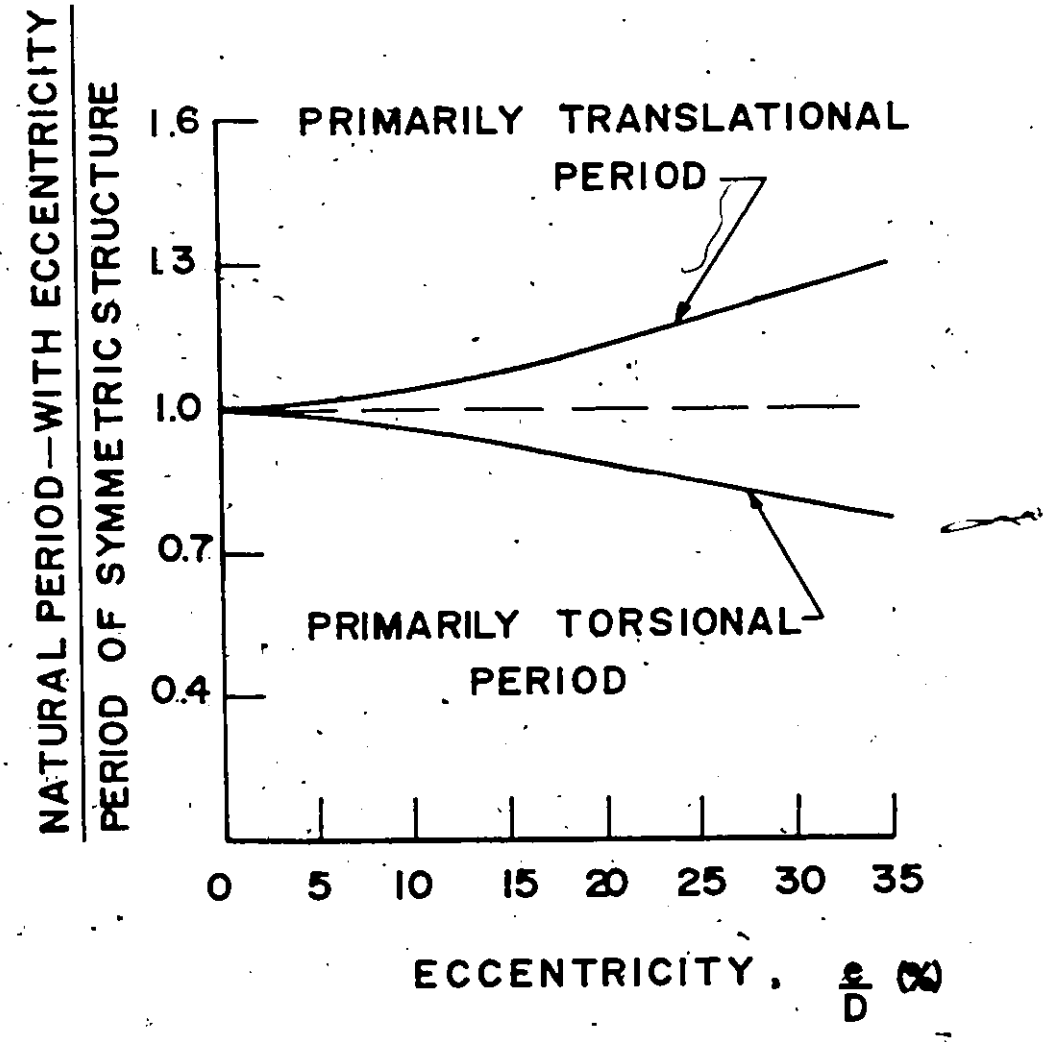

FIG. 3.3 EFFECT OF ECCENTRICITY ON NATURAL PERIODS

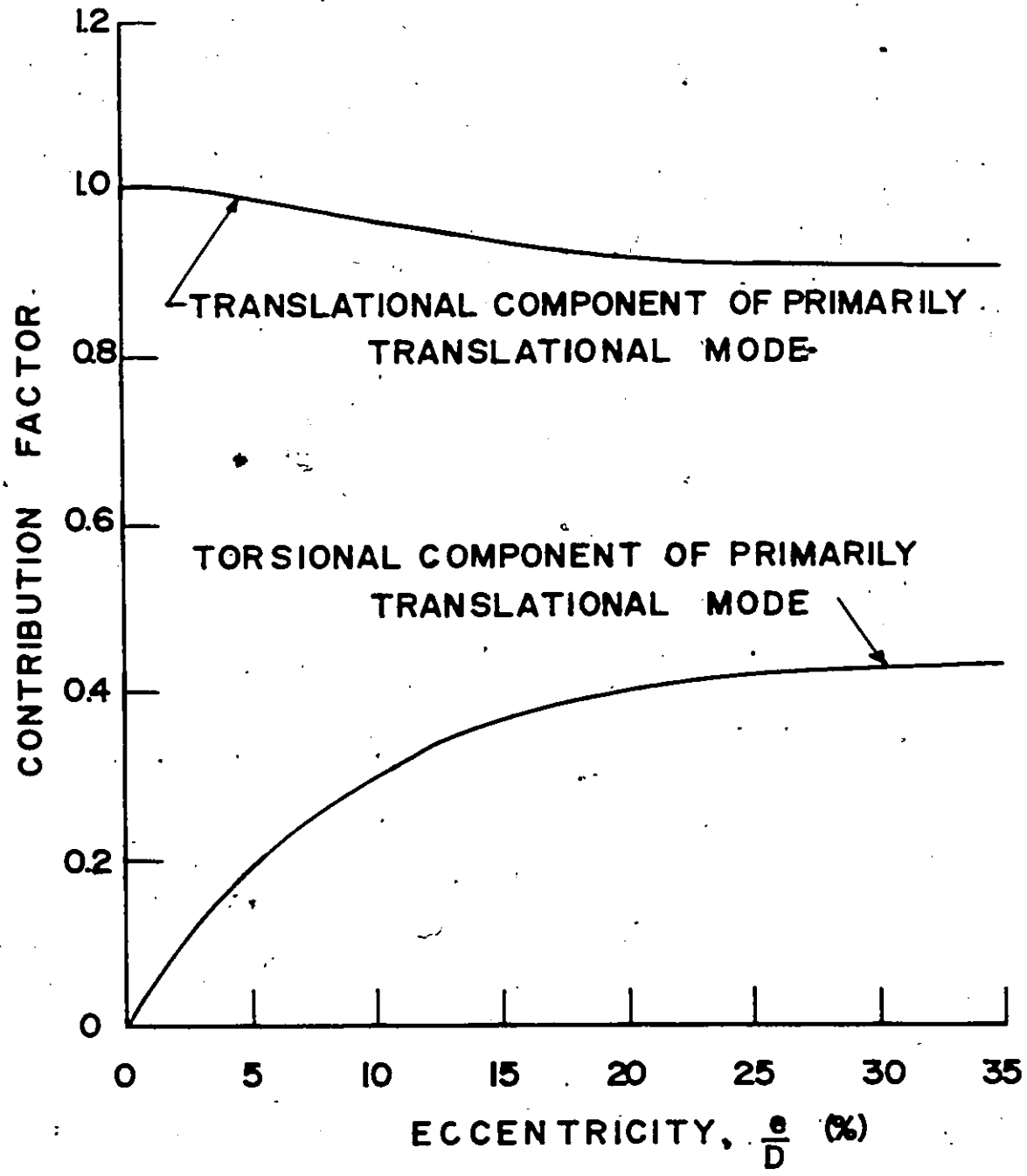

FIG. 3.4 EFFECT OF ECCENTRICITY ON FUNDAMENTAL TRANSLATIONAL MODE SHAPE

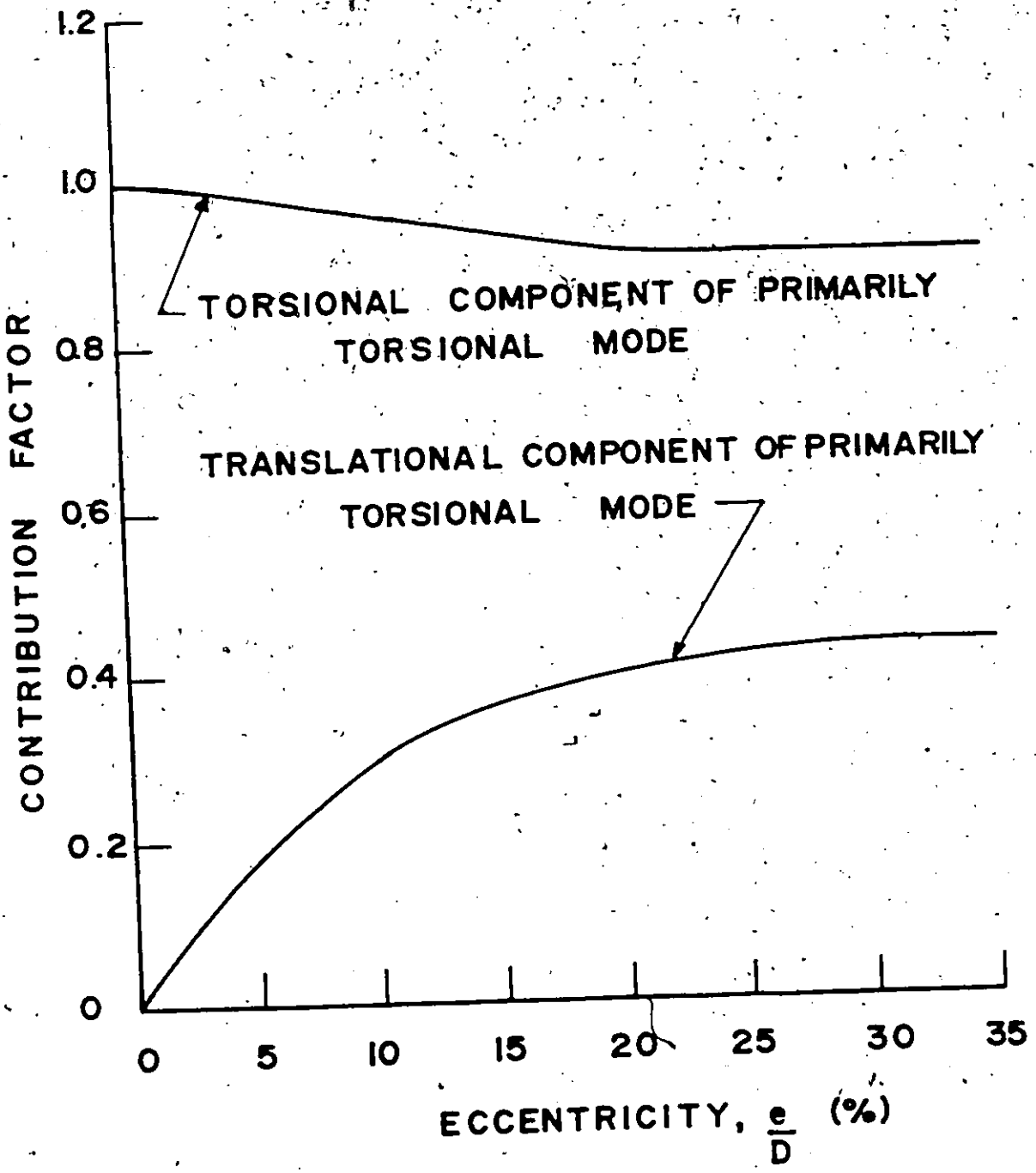

FIG. 3.5 EFFECT OF ECCENTRICITY ON FUNDAMENTAL TORSIONAL MODE SHAPE

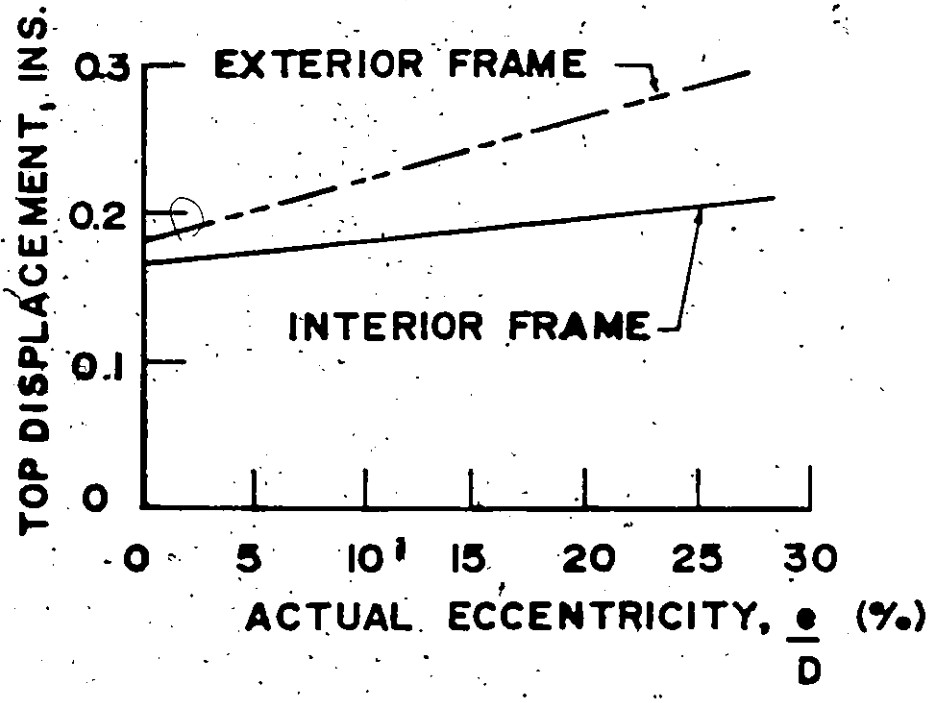

FIG. 3.6 CODE STATIC METHOD - TOP FLOOR DISPLACEMENT versus ECCENTRICITY

(ground acceleration 10% G, ductile space frame K=0.7)

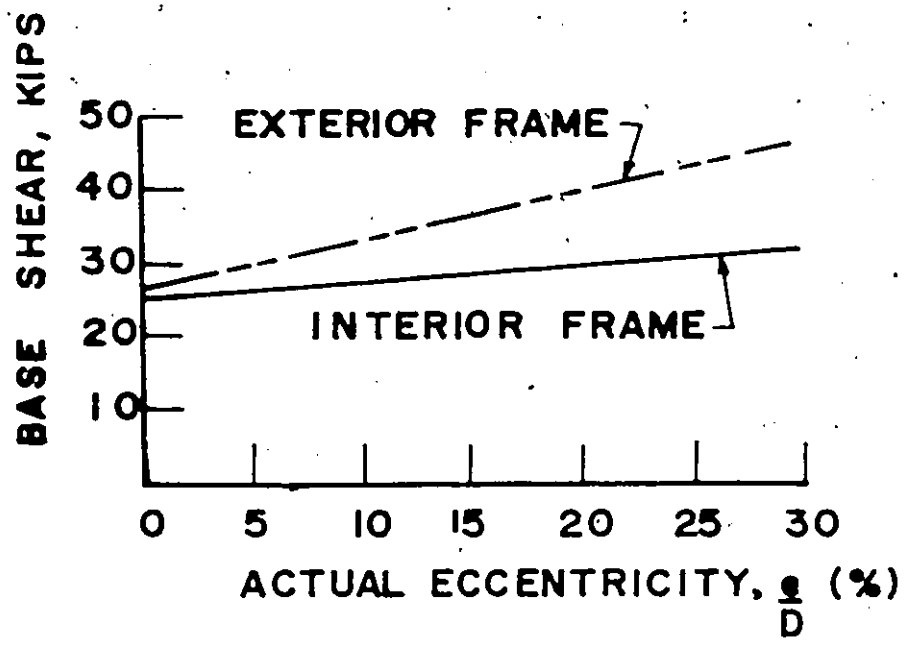

FIG. 3.7 CODE STATIC METHOD - FRAME BASE SHEAR versus ECCENTRICITY

(ground acceleration of 10% G, ductile space frame K=0.7)

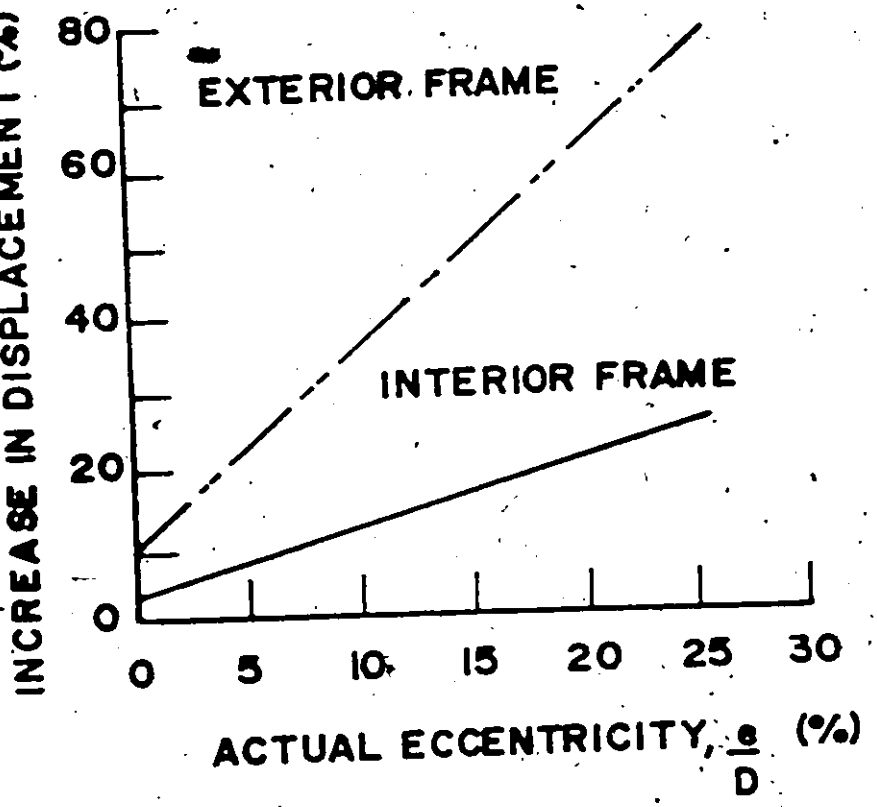

FIG. 3.8 PERCENT INCREASE IN DISPLACEMENT DUE TO ECCENTRICITY (See Fig. 3.6)

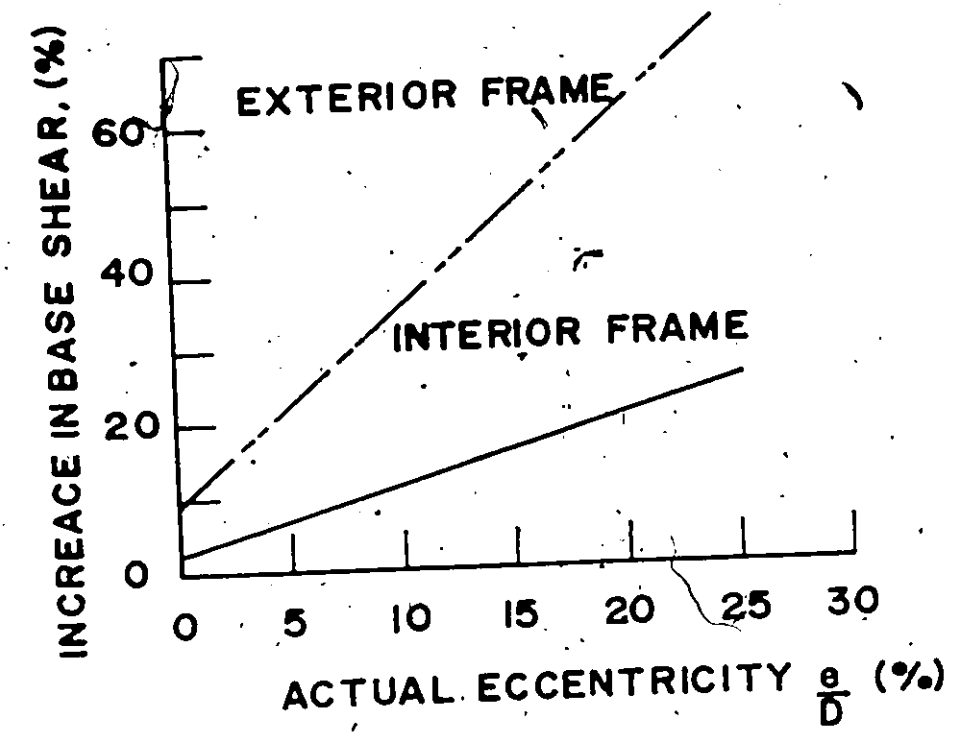

FIG. 3.9 PERCENT INCREASE IN BASE SHEAR DUE TO ECCENTRICITY (See Fig. 3.7)

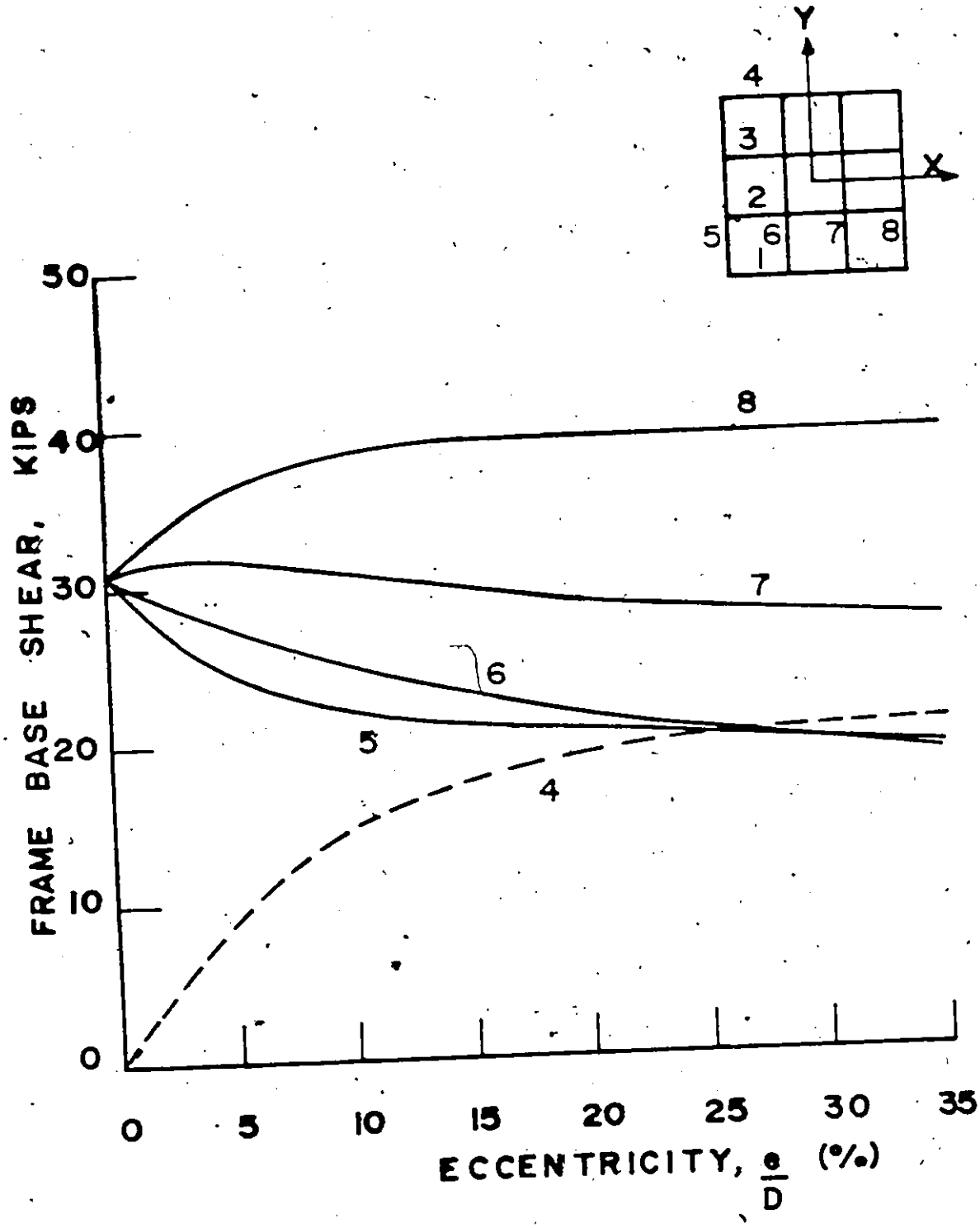

FIG. 3.10 EFFECT OF ECCENTRICITY ON FRAME BASE SHEAR-STIFF BUILDING (ground acceleration 10% G, ductility factor 0.4, 5% damping, symmetric translational period 0.5 sec.)

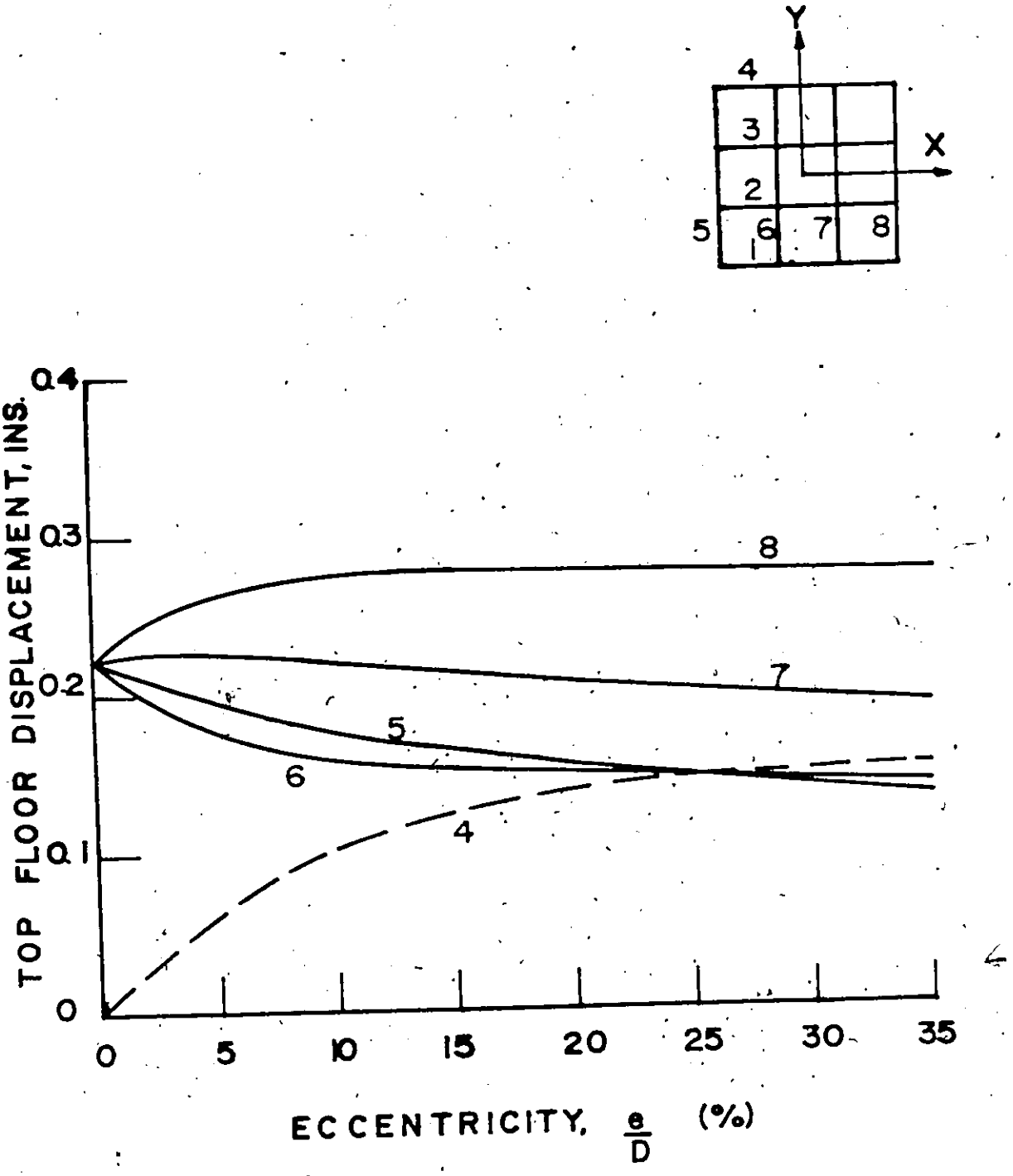

FIG. 3.11 EFFECT OF ECCENTRICITY ON TOP FLOOR DISPLACEMENT - STIFF BUILDING (ground acceleration 10% G, ductility factor 0.4, 5% damping, symmetric translational period 0.5 sec.)

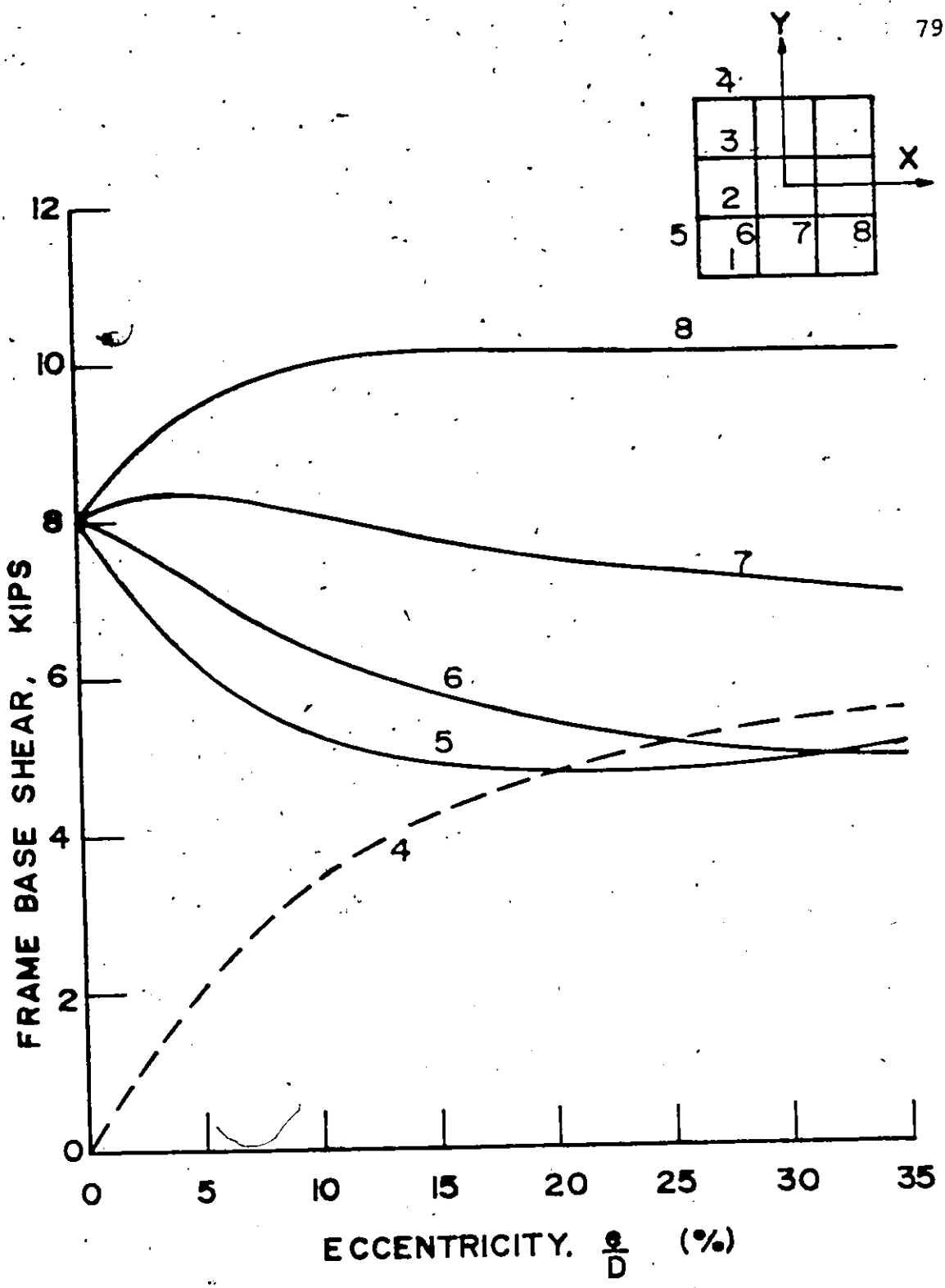

FIG. 3.12 EFFECT OF ECCENTRICITY ON FRAME BASE SHEAR-FLEXIBLE BUILDING (ground acceleration 10% G, ductility factor 0.4, 5% damping, symmetric translational period 0.5 sec.)

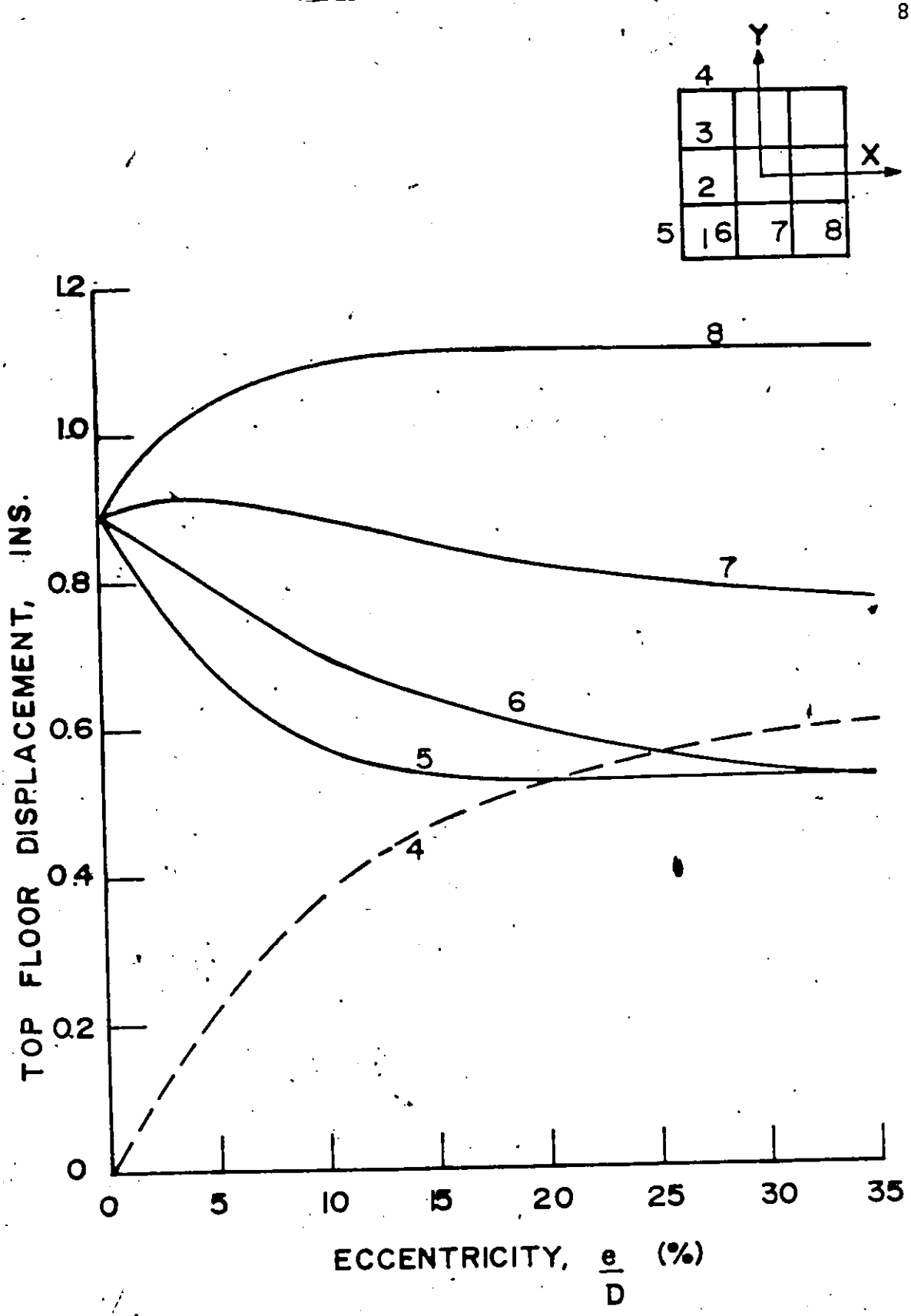

FIG. 3.13 EFFECT OF ECCENTRICITY ON TOP FLOOR DISPLACEMENT-FLEXIBLE BUILDING (ground acceleration 10% G; ductility factor 0.4, 5% damping, symmetric translational period 0.5 sec.)

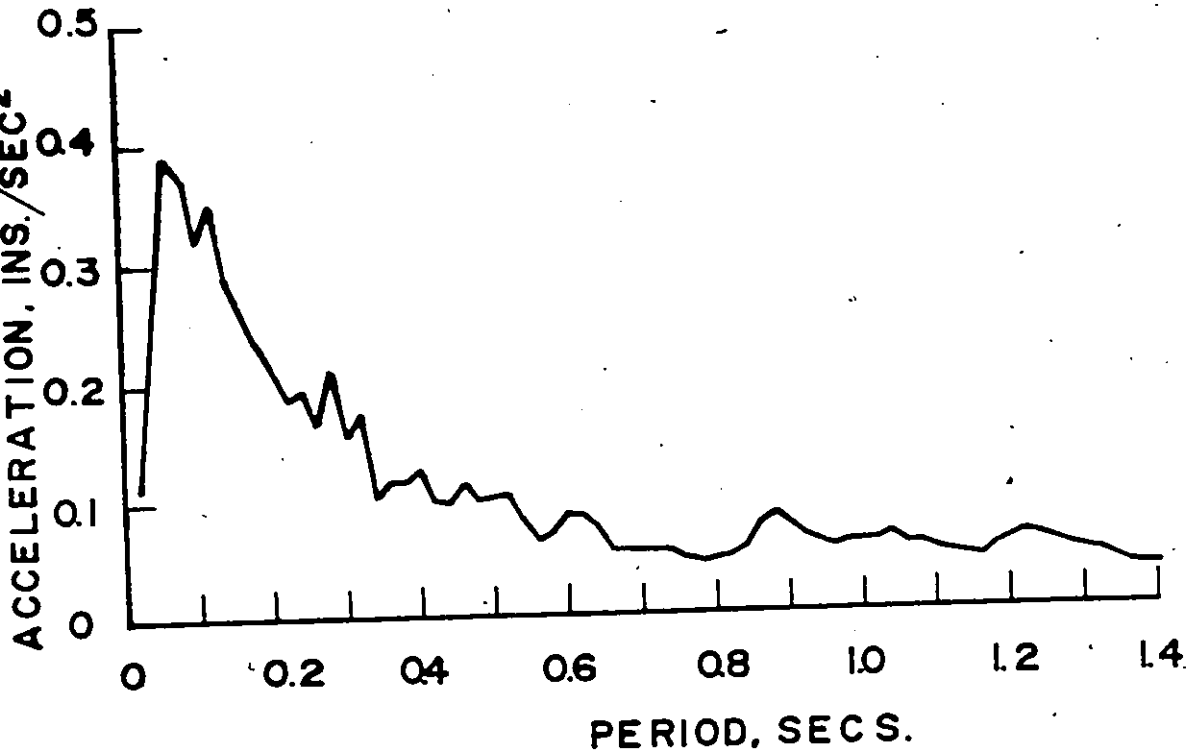

FIG. 4.1 ACCELERATION SPECTRUM - PSUEDO-EARTHQUAKE #1 (peak ground acceleration 10% G, build-up and decay times of 0.01 sec, 10 second record damping 0.6 and period 0.4 sec.)

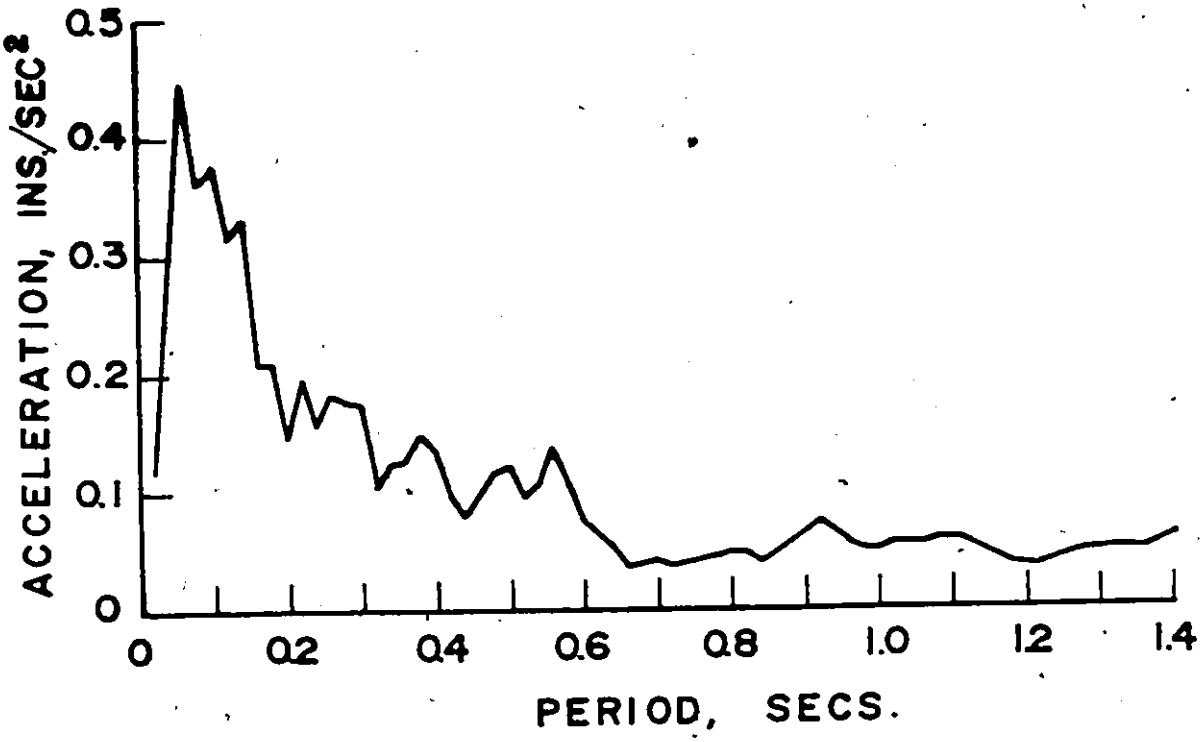

FIG. 4.2 ACCELERATION SPECTRUM - PSUEDO-EARTHQUAKE #2 (peak ground acceleration 10% G, build-up and decay times of 0.01 sec, 10 second record damping 0.6 and period 0.4 sec.)

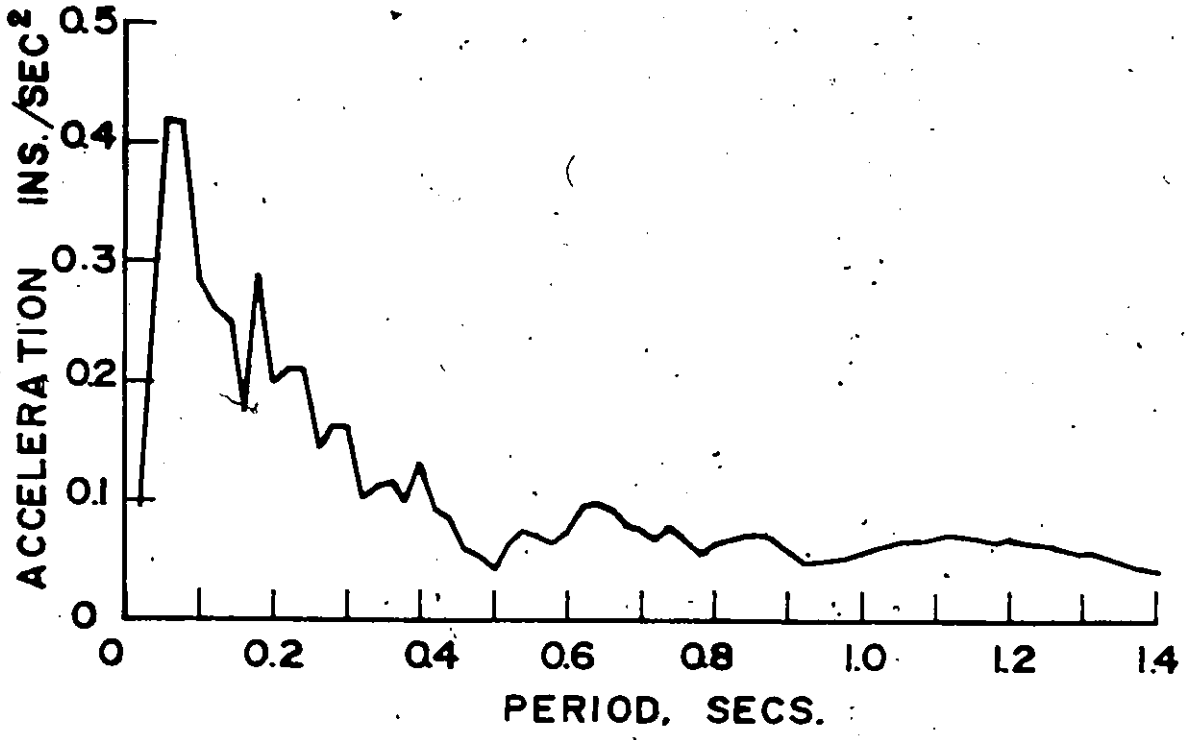

FIG. 4.3 ACCELERATION SPECTRUM - PSUEDO-EARTHQUAKE #3 (peak ground acceleration 10% G, build-up and decay times of 0.01 sec, 10 second record damping 0.6 and period 0.4 sec.)

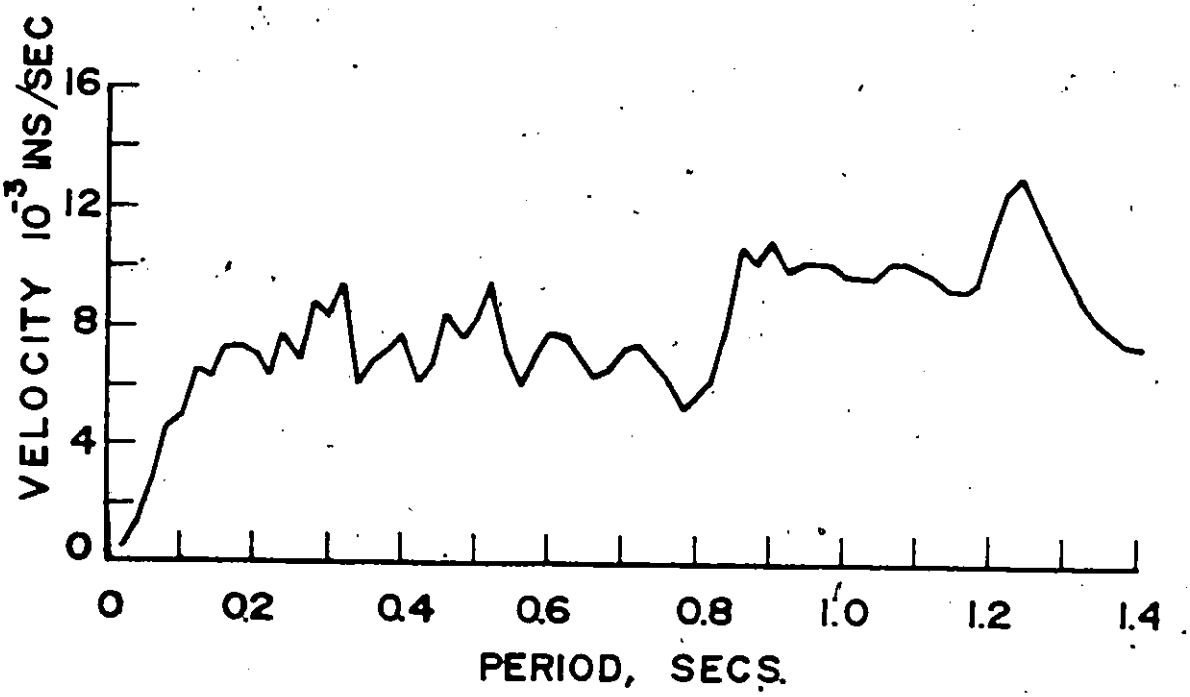

FIG. 4.4 VELOCITY SPECTRUM - PSUEDO EARTHQUAKE #1 (peak ground acceleration 10% G, build-up and decay times of 0.01 sec, 10 second record damping 0.6 and period 0.4 sec.)

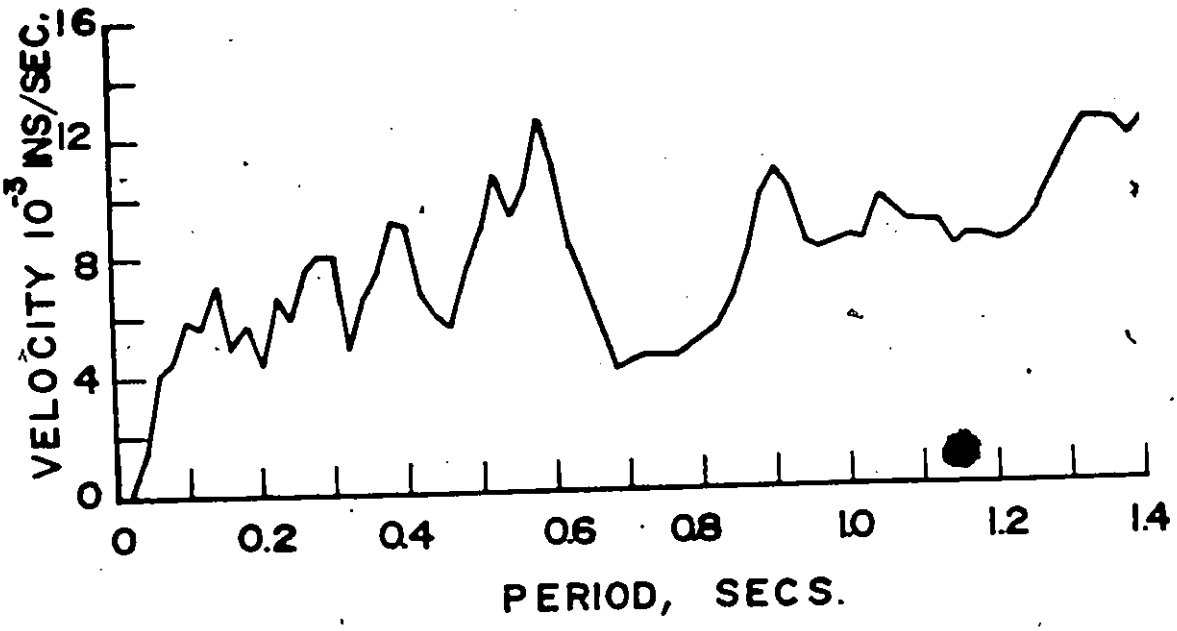

FIG. 4.5 VELOCITY SPECTRUM - PSUEDO EARTHQUAKE #2 (peak ground acceleration 10% G, build-up and decay times of 0.01 sec, 10 second record daming 0.6 and period 0.4 sec.)

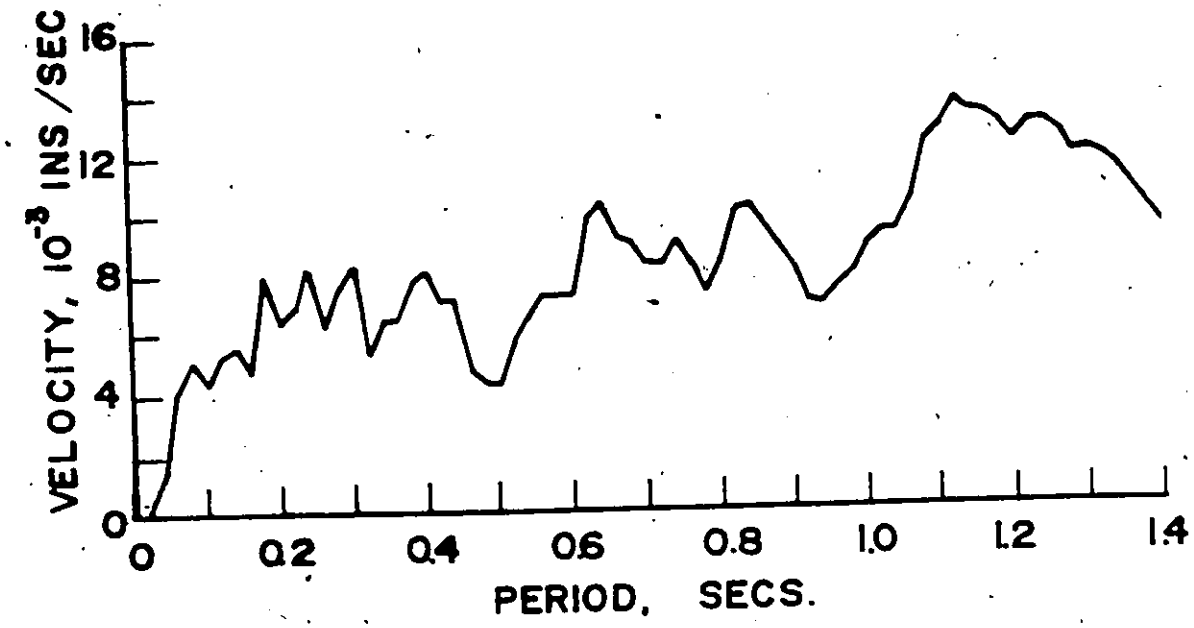

FIG. 4.6 VELOCITY SPECTRUM - PSUEDO EARTHQUAKE #3 (peak ground acceleration 10% G, build-up and decay times of 0.01 sec, 10 second record damping 0.6 and period 0.4 sec.)

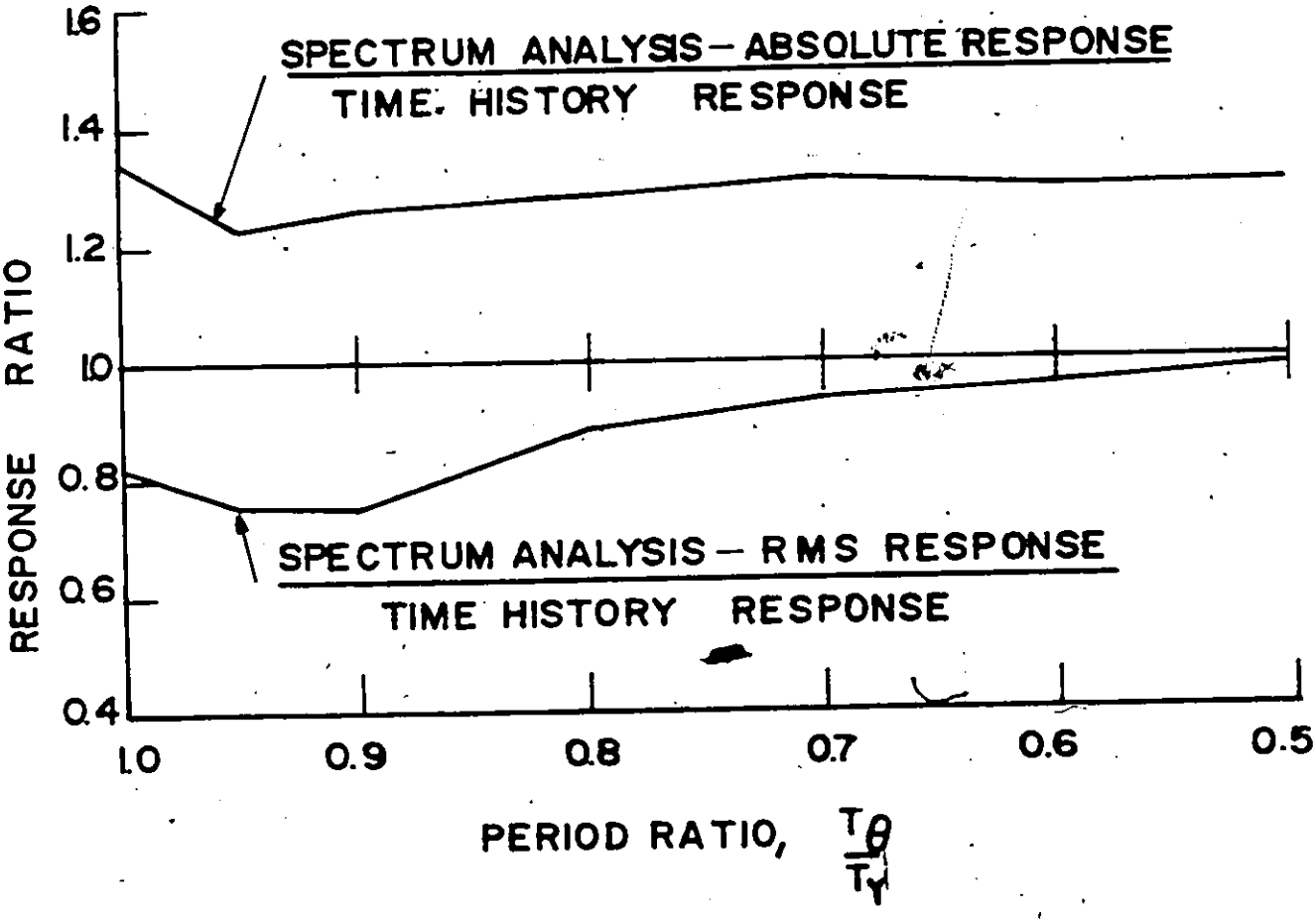

FIG. 4.7 EFFECT OF PERIOD COINCIDENCE ON COMPARISON OF RESPONSE SPECTRUM TECHNIQUES TO TIME HISTORY ANALYSIS - RIGID STRUCTURE (in terms of base shear of frames 5 to 8 and 3 psuedo-earthquakes, δ=0.1, damping=2%.)

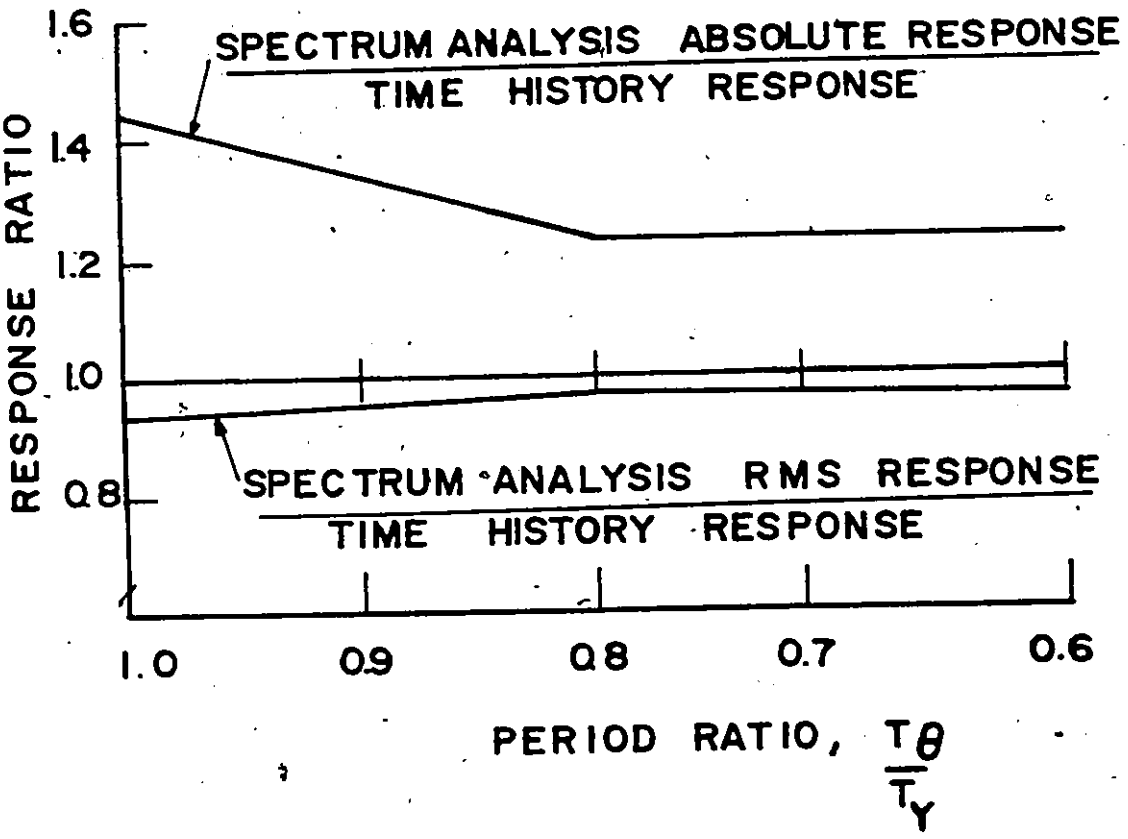

FIG. 4.8 EFFECT OF PERIOD COINCIDENCE ON COMPARISON OF RESPONSE TECHNIQUES TO TIME HISTORY ANALYSIS - FLEXIBLE STRUCTURE (in terms of base shear of frames 5 to 8 and 3 psuedo-earthquakes, δ=0.10, damping 2%.)

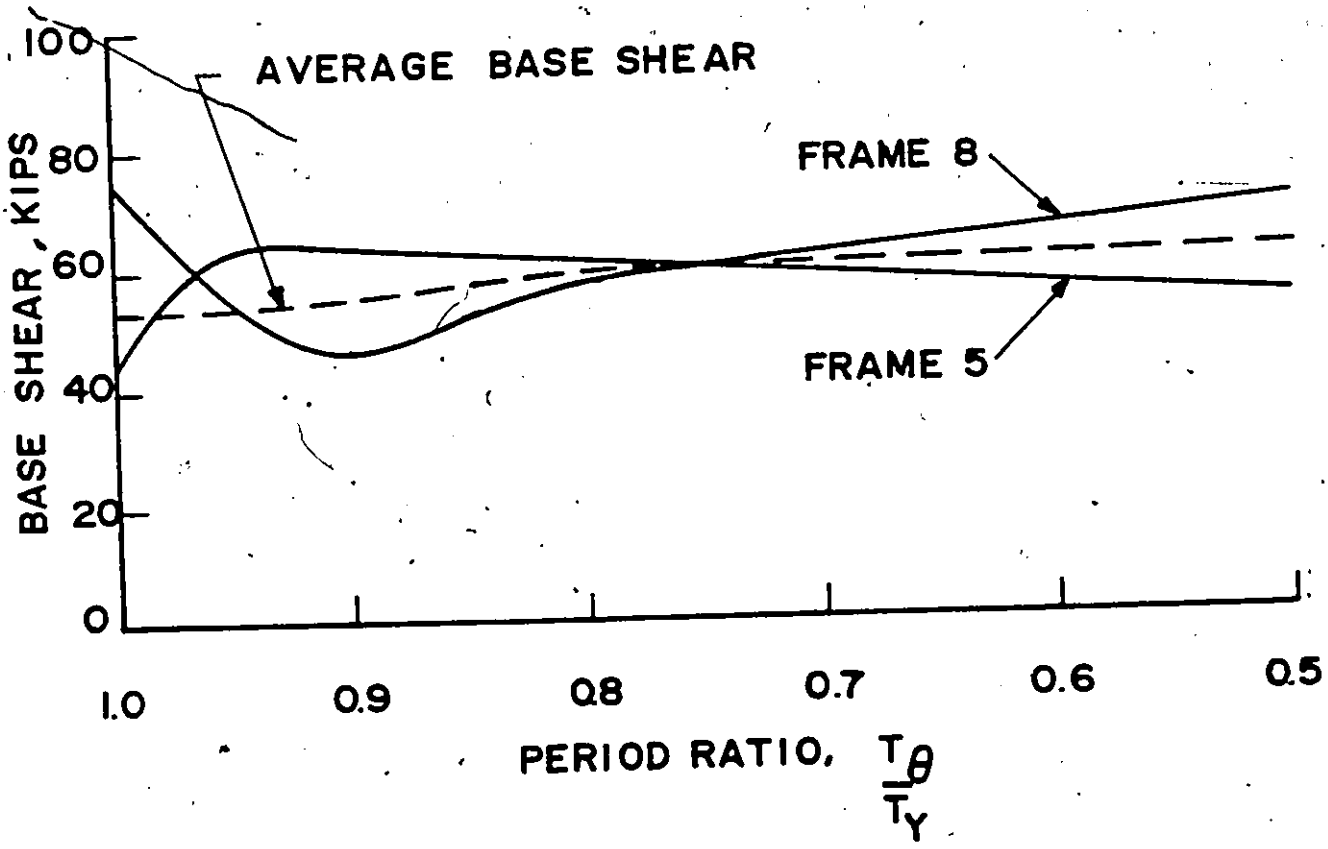

FIG. 4.9 EFFECT OF PERIOD SEPARATION ON BASE SHEAR OF EXTERNAL FRAMES - TIME HISTORY ANALYSIS (average of 3 psuedo-earthquakes δ=0.10, damping 2%.)

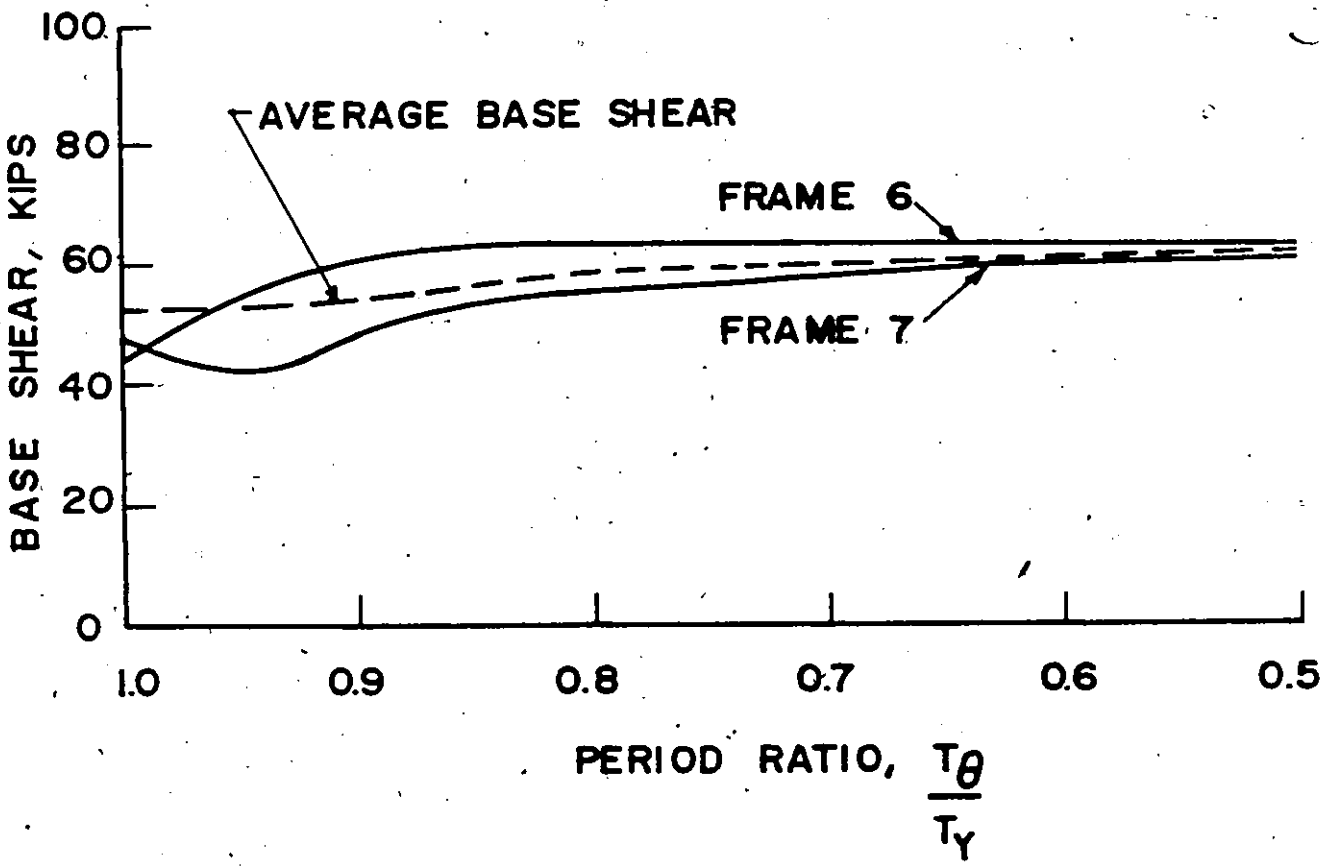

FIG. 4.10 EFFECT OF PERIOD SEPARATION ON BASE SHEAR OF INTERNAL FRAMES - TIME HISTORY ANALYSIS (average of 3 psuedo-earthquakes, δ=0.10, damping 2%.)

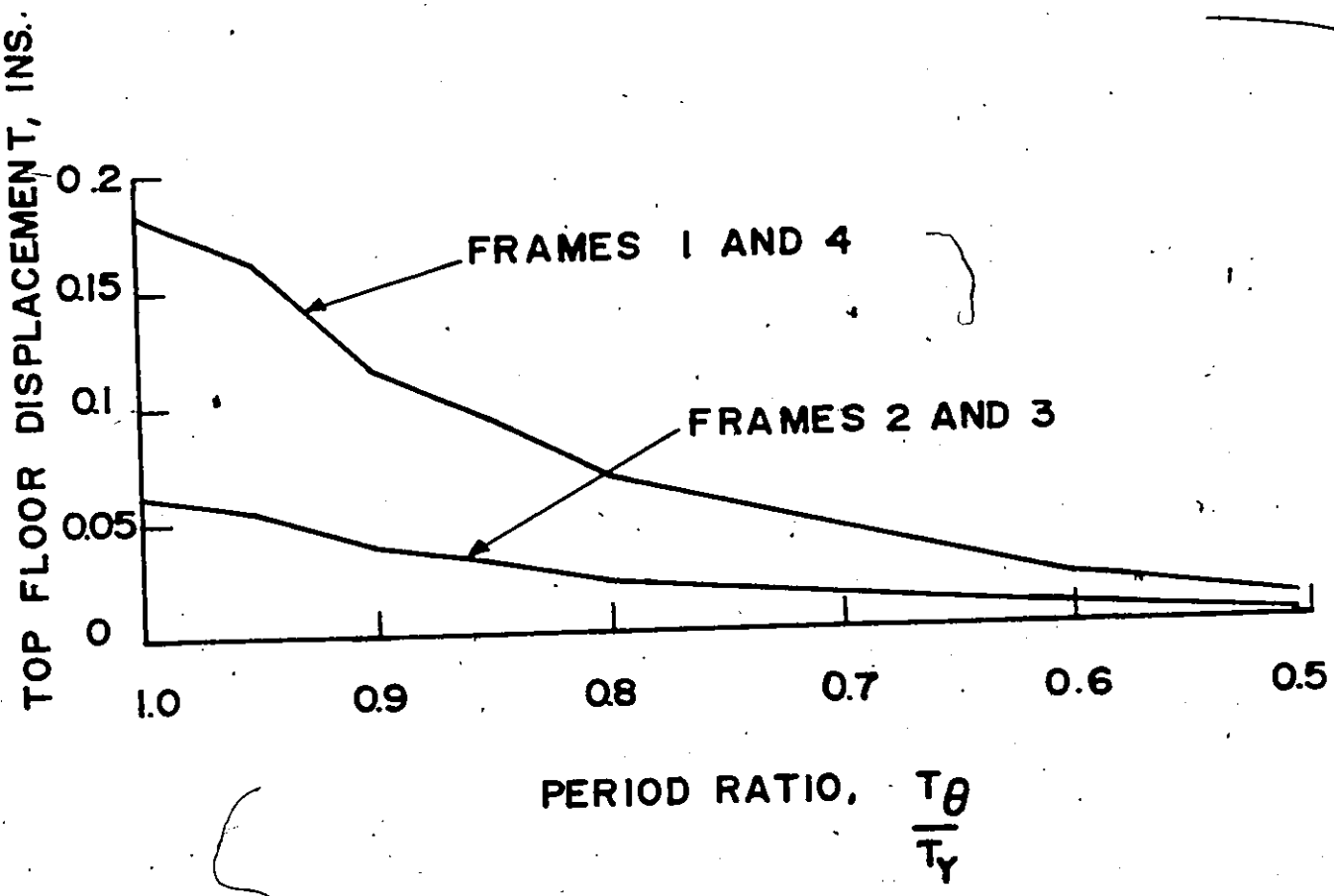

FIG. 4.11 EFFECT OF PERIOD SEPARATION ON TOP FLOOR DISPLACEMENT - TIME HISTORY ANALYSIS (average of 3 psuedo-earthquakes, δ=0.10, damping=2%.)

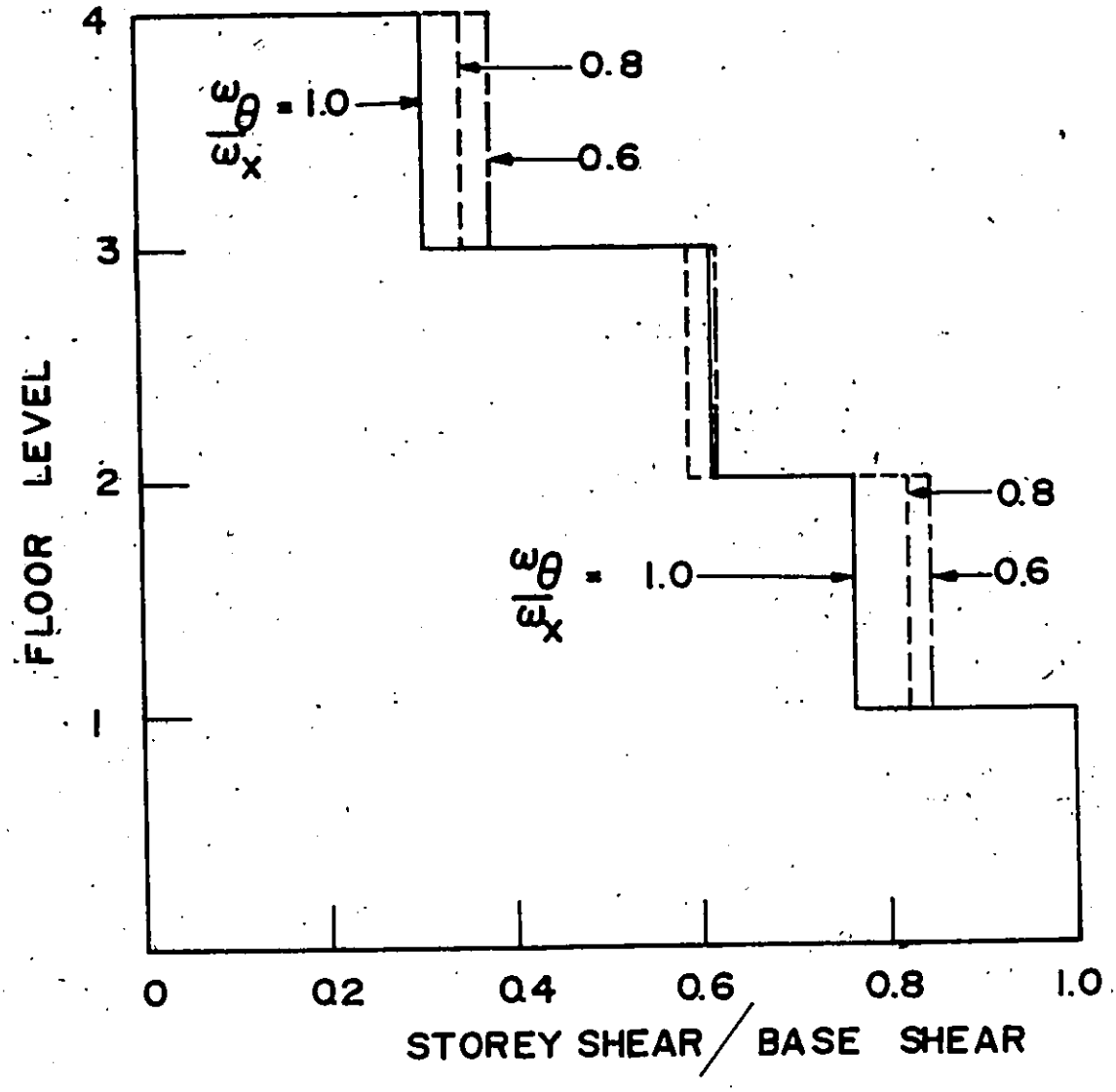

FIG. 4.12 EFFECT OF FREQUENCY RATIO ON DISTRIBUTION OF SHEAR (average shear distribution of frames 5 to 8, δ=0.10, damping=2%:)